

Article

# Polyfunctional Imidazolium Aryloxide Betaine / Lewis Acid Catalysts as Tool for the Asymmetric Synthesis of Disfavored Diastereomers

Felix Willig, Johannes Lang, Andreas C. Hans, Mark R Ringenberg, Daniel Pfeffer, Wolfgang Frey, and René Peters

*J. Am. Chem. Soc.*, **Just Accepted Manuscript** • DOI: 10.1021/jacs.9b04902 • Publication Date (Web): 03 Jul 2019

Downloaded from <http://pubs.acs.org> on July 3, 2019

## Just Accepted

"Just Accepted" manuscripts have been peer-reviewed and accepted for publication. They are posted online prior to technical editing, formatting for publication and author proofing. The American Chemical Society provides "Just Accepted" as a service to the research community to expedite the dissemination of scientific material as soon as possible after acceptance. "Just Accepted" manuscripts appear in full in PDF format accompanied by an HTML abstract. "Just Accepted" manuscripts have been fully peer reviewed, but should not be considered the official version of record. They are citable by the Digital Object Identifier (DOI®). "Just Accepted" is an optional service offered to authors. Therefore, the "Just Accepted" Web site may not include all articles that will be published in the journal. After a manuscript is technically edited and formatted, it will be removed from the "Just Accepted" Web site and published as an ASAP article. Note that technical editing may introduce minor changes to the manuscript text and/or graphics which could affect content, and all legal disclaimers and ethical guidelines that apply to the journal pertain. ACS cannot be held responsible for errors or consequences arising from the use of information contained in these "Just Accepted" manuscripts.

# Polyfunctional Imidazolium Aryloxide Betaine / Lewis Acid Catalysts as Tool for the Asymmetric Synthesis of Disfavored Diastereomers

Felix Willig,<sup>\*</sup> Johannes Lang,<sup>\*\*</sup> Andreas C. Hans,<sup>\*</sup> Mark R. Ringenberg,<sup>§</sup> Daniel Pfeffer,<sup>\*</sup> Wolfgang Frey,<sup>\*</sup> and René Peters<sup>\*\*</sup>

<sup>\*</sup> Institut für Organische Chemie, Universität Stuttgart, Pfaffenwaldring 55, D-70569 Stuttgart, Germany.

<sup>§</sup> Institut für Anorganische Chemie, Universität Stuttgart, Pfaffenwaldring 55, D-70569 Stuttgart, Germany.

**KEYWORDS:** cooperative catalysis; direct 1,4-additions; multifunctional catalysts; betaine; asymmetric catalysis

**ABSTRACT:** Enzymes are Nature's polyfunctional catalysts tailor-made for specific biochemical synthetic transformations, which often proceed with almost perfect stereocontrol. From a synthetic point of view, artificial catalysts usually offer the advantage of much broader substrate scopes, but stereocontrol is often inferior to enzymes. A particularly difficult synthetic task in asymmetric catalysis is to overwrite a pronounced preference for the formation of an inherently favored diastereomer and thus requires a particularly high level of stereocontrol. In this article, the development of a novel artificial polyfunctional catalyst type is described, in which an imidazolium-aryloxide betaine moiety cooperates with a Lewis acidic metal center (here Cu(II)) within a chiral catalyst framework. This strategy permitted for the first time a general, highly enantioselective access to the otherwise rare diastereomer in the direct 1,4-addition of various 1,3-dicarbonyl substrates to  $\beta$ -substituted nitroolefins. The unique stereocontrol by the polyfunctional catalyst system is also demonstrated with the highly stereoselective formation of a third contiguous stereocenter making use of a diastereoselective nitronate protonation employing  $\alpha,\beta$ -disubstituted nitroolefin substrates. Asymmetric 1,4-additions of  $\beta$ -ketoesters and  $\alpha,\beta$ -disubstituted nitroolefins have never been reported before. Combined mechanistic investigations including detailed spectroscopic and DFT studies suggest that the aryloxide acts as a base to form a Cu(II)-bound enolate, whereas the nitroolefin is activated by H-bonds to the imidazolium unit and the phenolic OH generated during the proton transfer. Detailed kinetic analyses (RPKA, VTNA) suggest that (a) the catalyst is stable during the catalytic reaction, (b) not inhibited by product and (c) the rate-limiting step is most likely the C-C bond formation in agreement with the DFT calculations of the catalytic cycle. The robust catalyst is readily synthesized, recyclable and could also be applied to a cascade cyclization.

## INTRODUCTION

Enzymes, the highly sophisticated catalysts that Nature has evolved over billions of years to regulate biochemical processes, make use of polyfunctional active sites. Many of them are capable of activating two substrates simultaneously by various active site functionalities.<sup>1</sup> Interaction of these enzyme functional groups with a proper nucleophile and a proper electrophile enables a precise spatial organization of both substrates within the chiral environment of the active site thus allowing for excellent stereoselectivities. Likewise, this cooperative mode of action leads to strongly increased reaction rates for the inherently favored substrates.<sup>1</sup>

For instance, class-II-aldolases constitute one of Nature's important tools to create C,C-bonds.<sup>2</sup> Scheme 1 (*top*) illustrates the suggested simplified operation mode of the polyfunctional active site of such a metal dependent enzyme, in which the bidentate pronucleophile forms a chelate complex with Zn(II).<sup>2</sup> This coordination further acidifies the  $\alpha$ -C,H-bond, which can thus be deprotonated by a Brønsted basic glutamate residue to generate a Zn-

enolate. The latter nucleophile attacks the aldehyde substrate that is activated by hydrogen bond formation with a tyrosine residue to form two stereocenters in this event.<sup>2</sup>

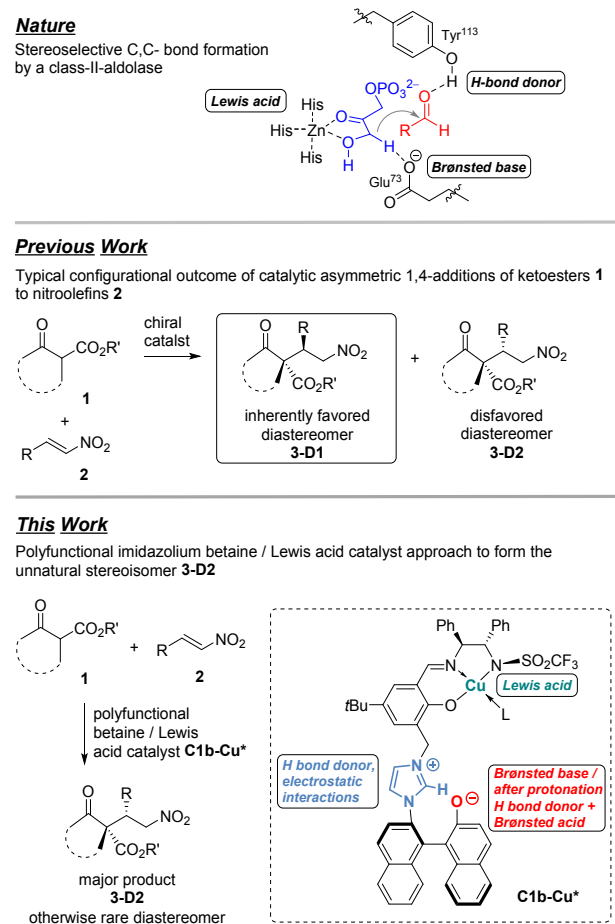
Because stereoisomers usually differ in their physiological properties,<sup>3</sup> a selective complementary access to different diastereomeric addition products is often desirable, in particular in medicinal chemistry. Achieving diastereodivergency in asymmetric catalysis is thus an important, but still very challenging synthetic task. Therefore various concepts, strategies and approaches have recently been developed to accomplish an efficient access to the otherwise rare diastereomers for various reaction types.<sup>4,5</sup>

Next to aldol additions, catalytic direct Michael-additions have been developed as efficient tools to construct C,C-bonds with adjacent stereocenters in an atom-economic and highly enantio- and diastereoselective fashion.<sup>6,7</sup> A synthetically attractive version is the direct conjugate addition of  $\beta$ -ketoesters to nitroolefins, because the carbonyl moieties as well as the nitro group offer many

options for further synthetic transformations.<sup>8,9</sup> Value-added 1,4-addition products to nitroolefins were applied to construct densely functionalized chiral products<sup>8</sup> including bioactive natural products and active pharmaceutical ingredients.<sup>10</sup>

Despite the large number of investigations dealing with the asymmetric addition of  $\alpha$ -substituted  $\beta$ -ketoesters **1** to nitroolefins **2**, the so far described catalysts have in common that for the overwhelming majority of reported substrate combinations –in particular for *all* cyclic  $\alpha$ -substituted  $\beta$ -ketoesters– the formation of the same relative product configuration is inherently strongly favored (Scheme 1, *middle*).<sup>8,11</sup> There is no general route yet toward the rare epimeric product series and hence epimeric follow-up products were not efficiently accessible so far.

**Scheme 1. Top: Operation Mode of the Active Site of a Class-II-Aldolase; Middle: Inherent Diastereoselectivity of the Title Reaction; Bottom: Use of an Artificial Polyfunctional Catalyst.**



In this article, an artificial polyfunctional catalyst type is reported in which similar tools as in enzymes (Lewis acid, Brønsted base, H-bond donors, ionic interactions), have been exploited to allow for an efficient enantioselective access toward the otherwise rare diastereomer in the addition of ketoesters **1** to nitroolefins **2**. In particular, this article introduces a novel cooperative catalysis strategy featuring the synergistic interplay between an

imidazolium aryloxide betaine moiety and a chiral Lewis acid fragment within the same catalyst framework (Scheme 1, bottom).<sup>12</sup> This polyfunctional catalyst is also shown to be capable of creating an additional stereocenter by stereoselective nitronate pronation using  $\alpha,\beta$ -disubstituted nitroolefins.

Ooi et al. could previously demonstrate the high potential of ammonium betaine organocatalysts in asymmetric synthesis.<sup>13</sup> We initially chose to study this polyfunctional catalyst approach based on the hypothesis that it might allow for a more or less independent spatial control over both reactants in the stereoselectivity determining transition state of the C-C bond formation in order to overwrite an inherent diastereoselectivity preference. Like in an aldolase, the pronucleophile should form a chelate complex with the metal center thus acidifying the  $\alpha$ -C,H-bond, which is then deprotonated by the basic naphtholate to form a metal enolate. On the other hand the electrophile should be activated by hydrogen bond formation with the generated naphthol/imidazolium moiety to synergistically facilitate the C-C-bond formation. Kinetic and computational investigations suggest that the stereoselectivity determining C-C-bond formation is also rate limiting.

## RESULTS AND DISCUSSION

### Catalyst Development and Optimization

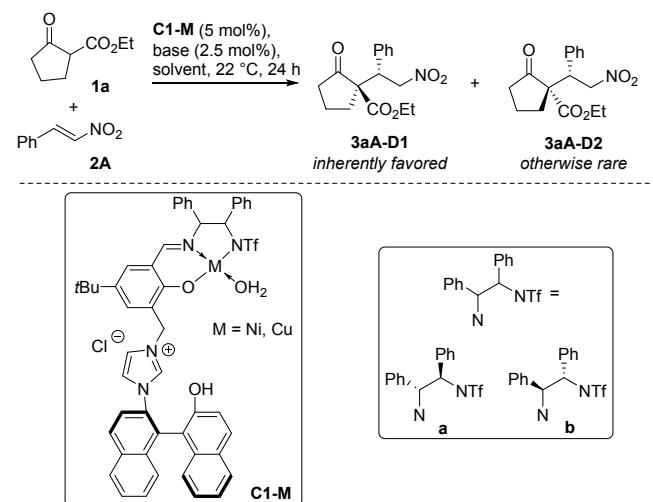
Bisimidazolium units have recently been explored by our group in cooperative asymmetric catalysis as H-bond donors,<sup>5k</sup> and because they might allow for additional  $\pi$ - or electrostatic interactions. The new precatalysts **C1-M** presented herein make use of an axially chiral binaphthyl unit carrying both an imidazolium and an acidic phenolic OH group. **C1a-Ni** and **C1b-Ni** (5 mol%) possessing different configurations of the iminotriflamide ligand fragment showed low activities (Table 1, entries 1 and 2), poor diastereo- but promising enantioselectivities. The activity could be increased by catalytic amounts of different bases (2.5 mol%). NEt<sub>3</sub>, Na(acac), and KOtBu all led to significant improvements in product yield and enantioselectivity (entries 3-5). With NEt<sub>3</sub> as the weakest base the smallest effect was found. For the other two bases the catalytic performance was very similar to each other, which pointed to the formation of the corresponding naphtholate of **C1b-Ni** as the catalytically active species. However, the preference for the otherwise rare diastereomer maintained at a low level. For that reason different metal centers M were installed and with copper(II) improved diastereoselectivity was attained. In the absence of base, only 13% of product was formed (entry 6). In the presence of Na(acac) as base, enantioselectivity and yield were again significantly improved (entry 8). Albeit catalyst **C1b-Cu** is not performing as rapid as its Ni-counterpart, the diastereoselectivity favoring the otherwise rare diastereomer **3aA-D2** was significantly higher.

NEt<sub>3</sub> was again a less efficient base in terms of product yield and enantioselectivity, but also regarding the diastereoselectivity (entry 7). Also with KOtBu the diastereoselectivity was initially smaller (entry 9). In general we found that the base amount is a critical factor. Since 5 mol% of the polyfunctional catalyst were used, but just 2.5 mol% of base, only half of it would be in the more

active and selective betaine form. On the other hand, increasing the base loadings led to reproducibility problems, which were explained by unreacted free base leading to background reactions. Switching to THF as solvent (entry 10) had a positive effect on the base solubility and reproducibility.

To avoid free unreacted base, the betaine catalyst **C1b-Cu\*** was then preformed by filtration of **C1b-Cu** over basic silica gel with CH<sub>2</sub>Cl<sub>2</sub>/THF/NEt<sub>3</sub> (66:33:1) as eluent. This proceeding provided reproducible data (entry 11). The diastereomeric catalyst **C1a-Cu\*** provided the optical antipode of the rare product diastereomer **3aA-D2** with high selectivity (entry 12).

**Table 1. Development of a Catalyst to Form the Otherwise Rare Diastereomer 3aA-D2.**



| #  | catalyst       | base                   | solvent                         | yield (%) <sup>a</sup> | D1:D2 <sup>a</sup> | ee (%) <sup>b</sup> |
|----|----------------|------------------------|---------------------------------|------------------------|--------------------|---------------------|
| 1  | <b>C1a-Ni</b>  | -                      | CH <sub>2</sub> Cl <sub>2</sub> | 11                     | 40:60              | -51                 |
| 2  | <b>C1b-Ni</b>  | -                      | CH <sub>2</sub> Cl <sub>2</sub> | 35                     | 43:57              | 63                  |
| 3  | <b>C1b-Ni</b>  | NEt <sub>3</sub>       | CH <sub>2</sub> Cl <sub>2</sub> | 77                     | 38:62              | 91                  |
| 4  | <b>C1b-Ni</b>  | Na(acac)               | CH <sub>2</sub> Cl <sub>2</sub> | 93                     | 38:62              | 97                  |
| 5  | <b>C1b-Ni</b>  | KOtBu                  | CH <sub>2</sub> Cl <sub>2</sub> | 94                     | 35:65              | 98                  |
| 6  | <b>C1b-Cu</b>  | -                      | CH <sub>2</sub> Cl <sub>2</sub> | 13                     | 32:68              | 74                  |
| 7  | <b>C1b-Cu</b>  | NEt <sub>3</sub>       | CH <sub>2</sub> Cl <sub>2</sub> | 34                     | 21:79              | 92                  |
| 8  | <b>C1b-Cu</b>  | Na(acac)               | CH <sub>2</sub> Cl <sub>2</sub> | 62                     | 13:87              | 96                  |
| 9  | <b>C1b-Cu</b>  | KOtBu                  | CH <sub>2</sub> Cl <sub>2</sub> | 20                     | 24:76              | 78                  |
| 10 | <b>C1b-Cu</b>  | KOtBu                  | THF                             | 78                     | 11:89              | 97                  |
| 11 | <b>C1b-Cu*</b> | preactiv. <sup>c</sup> | THF                             | 88                     | 11:89              | 97                  |
| 12 | <b>C1a-Cu*</b> | preactiv. <sup>c</sup> | THF                             | 98                     | 9:91               | -87                 |

<sup>a</sup> Determined by <sup>1</sup>H NMR analysis of the crude product using mesitylene as an internal standard. <sup>b</sup> Enantiomeric excess of the major diastereomer **3aA-D2** determined by HPLC. A minus sign indicates that the other enantiomer than the one depicted was produced in excess. <sup>c</sup> The catalyst was preactivated forming betaine **C1-Cu\*** by filtration over silica gel using with CH<sub>2</sub>Cl<sub>2</sub>/THF/NEt<sub>3</sub> (66:33:1) as eluent.

High diastereoselectivities were attained by performing the reaction at -20 °C (Table 2). For high yields it was

necessary to increase the concentration (compare entries 1 & 2). High yields with lower catalyst loadings were accomplished under neat reaction conditions, in which the ketoester (1.5-2 equiv) also acts as solvent (entries 3-5). With 0.5 mol% of catalyst it was possible to form the product in 89% yield with a dr of 94:6 favoring the otherwise rare diastereomer D2 in almost enantiopure form (99% ee, entry 5).

**Table 2. Optimization of Reaction Conditions.**

| # | x   | equiv. 1a | c (X, mol/L) | t (h) | yld. (%) <sup>a</sup> | D1:D2 <sup>a</sup> | ee (%) <sup>b</sup> |
|---|-----|-----------|--------------|-------|-----------------------|--------------------|---------------------|
| 1 | 5.0 | 1.1       | 0.2          | 24    | 73                    | 5:95               | 96                  |
| 2 | 5.0 | 1.1       | 0.5          | 24    | 92                    | 4:96               | 97                  |
| 3 | 1.0 | 1.5       | neat         | 24    | 85                    | 6:94               | 98                  |
| 4 | 0.5 | 2         | neat         | 24    | 65                    | 6:94               | 99                  |
| 5 | 0.5 | 2         | neat         | 72    | 89                    | 6:94               | 99                  |

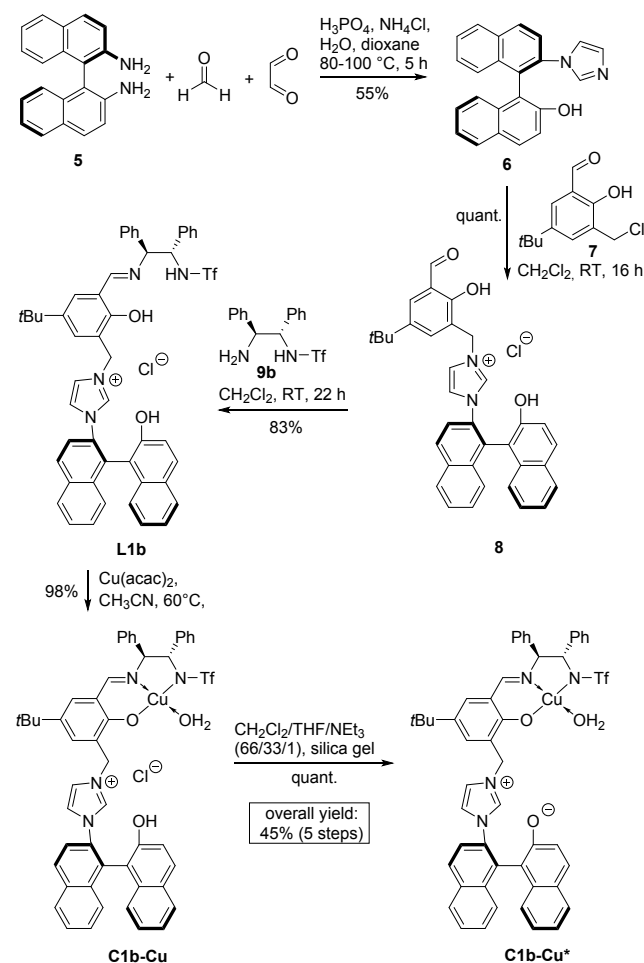
<sup>a</sup> Determined by <sup>1</sup>H NMR analysis of the crude product using mesitylene as an internal standard. <sup>b</sup> Enantiomeric excess of **3aA-D2** determined by HPLC.

### Catalyst Synthesis

The catalyst synthesis is based on the transformation of commercially available BINAM (**5**) with paraformaldehyde and glyoxal in the presence of phosphoric acid, water and ammonium chloride into the bifunctional naphthol/imidazole building block **6**, which was previously described by Crabtree *et al.*<sup>14</sup> Further optimization of this procedure provided **6** in useful yield (Scheme 2).

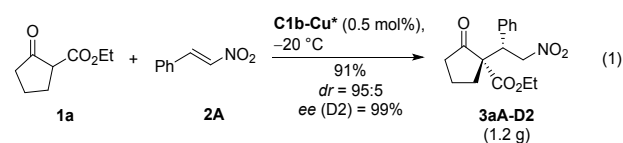
Subsequent alkylation of **6** with the known benzylic chloride **7**<sup>15</sup> under S<sub>N</sub>2 conditions and then imine formation with amine **9b** proceeded smoothly.<sup>16</sup> The yellow colored ligand **L1b** was then treated with Cu(acac)<sub>2</sub> providing the olive-green Cu(II) complex **C1b-Cu**. The active, red-brown colored betaine form was obtained by filtration over basic silica gel as described above. The last two steps proceeded in quasi-quantitative yield and delivered paramagnetic **C1b-Cu** and **C1b-Cu\*** in pure form as judged by microanalysis, mass spectrometry and UV-Vis spectroscopy. Overall the synthesis took 5 steps and the overall yield was 45%. The catalyst synthesis strategy is modular and applicable to various catalyst derivatives, as exemplified for the synthesis of the control catalyst systems **C3-C8** (Supporting Information, for the structures see below in Table 6).

## Scheme 2. Synthesis of Betaine Catalyst C1b-Cu\*.



## Scope

The model reaction was also investigated on a gram scale (eq. 1). With 0.5 mol% of preactivated catalyst **C1b-Cu\*** under solvent-free conditions 1.2 g of almost enantiopure product was isolated (91% yield) with a dr of 95:5.



The title reaction could also be applied to a number of different nitroolefins **2** providing similar results (Table 3). In all cases, the otherwise rare diastereomer was formed in excess - usually with high diastereo- and enantioselectivity and high to excellent yields. On aromatic residues R  $\sigma$ -acceptors like Br and Cl atoms (entries 2-7),  $\pi$ -acceptors like a nitro group (entries 8-10),  $\sigma$ -donors like a methyl group (entries 11-13), and  $\pi$ -donors like a methoxy group (entries 14, 16) were all well

tolerated. The same can be stated for different kinds of substituents in *para* (entries 2, 5, 8, 11, 14, 17), *meta* (entries 3, 6, 9, 12, 15, 17) and *ortho* (entries 4, 7, 10, 13, 16) positions. In the latter case, the largest variation of the dr value ranging from 10:90 (entry 4) to 1:99 (entry 10) was noted, whereas in the case of *meta* and *para* substitution dr values were close to 5:95. Moreover, heteroaromatic residues R were well accommodated (entries 18 and 19).

**Table 3. Application to Different Nitroolefins.**

| #               | R  | 3a         | yield (%) <sup>a</sup> | D1 : D2 <sup>a</sup> | ee (%) <sup>b</sup> |
|-----------------|--|------------|------------------------|----------------------|---------------------|
| 1               | Ph   | <b>3aA</b> | 99                     | 6 : 94               | 99                  |
| 2               | <i>p</i> -Br-C <sub>6</sub> H <sub>4</sub>               | <b>3aB</b> | 91                     | 6 : 94               | 99                  |
| 3               | <i>m</i> -Br-C <sub>6</sub> H <sub>4</sub>               | <b>3aC</b> | 96                     | 4 : 96               | 99                  |
| 4               | <i>o</i> -Br-C <sub>6</sub> H <sub>4</sub>               | <b>3aD</b> | 83                     | 10 : 90              | 99                  |
| 5               | <i>p</i> -Cl-C <sub>6</sub> H <sub>4</sub>               | <b>3aE</b> | 98                     | 5 : 95               | 99                  |
| 6               | <i>m</i> -Cl-C <sub>6</sub> H <sub>4</sub>               | <b>3aF</b> | 96                     | 3 : 97               | 99                  |
| 7               | <i>o</i> -Cl-C <sub>6</sub> H <sub>4</sub>               | <b>3aG</b> | 83                     | 7 : 93               | 99                  |
| 8               | <i>p</i> -O <sub>2</sub> N-C <sub>6</sub> H <sub>4</sub> | <b>3aH</b> | >99                    | 6 : 94               | 98                  |
| 9               | <i>m</i> -O <sub>2</sub> N-C <sub>6</sub> H <sub>4</sub> | <b>3aI</b> | >99                    | 3 : 97               | 99                  |
| 10              | <i>o</i> -O <sub>2</sub> N-C <sub>6</sub> H <sub>4</sub> | <b>3aJ</b> | 97                     | 1 : 99               | 99                  |
| 11              | <i>p</i> -Me-C <sub>6</sub> H <sub>4</sub>               | <b>3aK</b> | 92                     | 7 : 93               | 99                  |
| 12              | <i>m</i> -Me-C <sub>6</sub> H <sub>4</sub>               | <b>3aL</b> | 97                     | 4 : 96               | 99                  |
| 13              | <i>o</i> -Me-C <sub>6</sub> H <sub>4</sub>               | <b>3aM</b> | 85                     | 4 : 96               | 99                  |
| 14              | <i>p</i> -MeO-C <sub>6</sub> H <sub>4</sub>              | <b>3aN</b> | 90                     | 7 : 93               | 99                  |
| 15              | <i>m</i> -MeO-C <sub>6</sub> H <sub>4</sub>              | <b>3aO</b> | 95                     | 4 : 96               | 99                  |
| 16              | <i>o</i> -MeO-C <sub>6</sub> H <sub>4</sub>              | <b>3aP</b> | 79                     | 5 : 95               | 99                  |
| 17              |  | <b>3aQ</b> | 94                     | 5 : 95               | 99                  |
| 18              | 2-furyl  | <b>3aR</b> | 90                     | 10 : 90              | 99                  |
| 19              | 2-thiophenyl   | <b>3aS</b> | 97                     | 4 : 96               | 98                  |
| 20              |  | <b>3aT</b> | 85                     | 9 : 91               | 97                  |
| 21              | <i>i</i> Pr  | <b>3aU</b> | 92                     | 2 : 98               | 99                  |
| 22 <sup>c</sup> | cyclo-Hex  | <b>3aV</b> | 90                     | 3 : 97               | 99                  |
| 23 <sup>c</sup> | cyclo-Pr   | <b>3aW</b> | 96                     | 12 : 88              | 98                  |
| 24 <sup>c</sup> | <i>i</i> Bu  | <b>3aX</b> | 86                     | 10 : 90              | 99                  |
| 25 <sup>c</sup> | <i>n</i> Pr  | <b>3aY</b> | 96                     | 13 : 87              | 98                  |
| 26              |  | <b>3aZ</b> | 56                     | 26 : 74              | 96                  |

<sup>a</sup> Yield of isolated product as diastereomeric mixture after column chromatography. Diastereomeric ratios were determined from the crude product by <sup>1</sup>H-NMR. <sup>b</sup> Enantiomeric excess of **3a-D2** determined by HPLC. <sup>c</sup> Reaction performed under neat conditions.

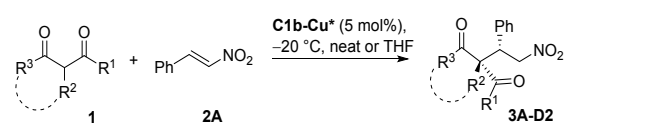
The reaction is also applicable to a  $\gamma,\delta$ -unsaturated nitroolefin, *i.e.* a conjugated diene, and proceeded with

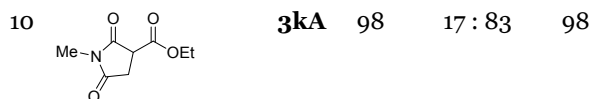
good yield, diastereoselectivity, excellent enantioselectivity and complete regioselectivity (entry 20). A possible 1,6-addition product was not detected.

The reaction is also attractive for nitroolefins carrying alkyl substituents. With the  $\alpha$ -branched isopropyl and cyclohexyl residues the otherwise rare diastereomers were formed with high diastereoselectivity, yield and enantioselectivity (entries 21 and 22). Good diastereoselectivity was also attained with substrates bearing cyclopropyl and isobutyl substituents (entries 23 and 24). In addition, linear alkyl groups like *n*-propyl residues are well tolerated despite the relatively high C-H acidity at the  $\gamma$ -position (entry 25). For entry 26, R is an ester moiety, leading to product **3aZ** containing a configurationally potentially labile stereocenter. Nevertheless, the rare diastereomer was still formed in access with high enantioselectivity under the mild reaction conditions.

Overall, in all 26 cases almost enantiopure product was formed. Additionally, the reaction was applied to different 1,3-dicarbonyl substrates as pronucleophiles (Table 4).<sup>17,18</sup>

**Table 4. Application to Different Pronucleophiles.**

|  |  |            |                        |                      |                     |
|---|--|------------|------------------------|----------------------|---------------------|
| #   |  | <b>3</b>   | yield (%) <sup>a</sup> | D1 : D2 <sup>a</sup> | ee (%) <sup>b</sup> |
| 1   |  | <b>3bA</b> | 92                     | 5 : 95               | 99                  |
| 2   |  | <b>3cA</b> | 92                     | 3 : 97               | 99                  |
| 3   |  | <b>3dA</b> | 89                     | 7 : 93               | 99                  |
| 4 <sup>c</sup>  |  | <b>3eA</b> | 96                     | 20 : 80              | 97                  |
| 5   |  | <b>3fA</b> | 96                     | 9 : 91               | 99                  |
| 6   |  | <b>3gA</b> | 54                     | 31 : 69              | 92                  |
| 7   |  | <b>3hA</b> | 82                     | 16 : 84              | 75                  |
| 8   |  | <b>3iA</b> | 58                     | -                    | 80                  |
| 9 <sup>d</sup>  |  | <b>3jA</b> | 71                     | 16 : 84              | 91                  |



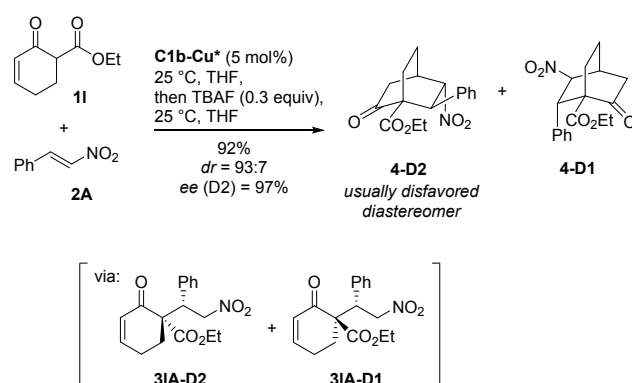
<sup>a</sup>Yield of isolated product after column chromatography as diastereomeric mixture. <sup>b</sup> Enantiomeric excess of **3a-D2** determined by HPLC. <sup>c</sup> The reaction was performed at 0 °C. <sup>d</sup> The reaction was performed at -30 °C.

Variation of the ester substituent at the cyclopentanone ring had no large impact on stereoselectivity and yield. With the more bulky isopropyl ester group the preference for the otherwise rare diastereomer became a bit higher (compare entry 2 with entry 1 and Table 3, entry 1). Nevertheless, all other examples in Table 4 made use of Me or Et esters. An indanone derivative was also well accommodated (entry 3). Six-, seven- and eight-membered rings were also tolerated and high enantioselectivity was attained in all cases (entries 4-6). For the less reactive cyclohexanone and -octanone the diastereoselectivity was moderate, but the otherwise rare product diastereomers were still favored. With an acyclic ketoester, the enantioselectivity was lower than with the cyclic ones (entry 7).<sup>19</sup> The experiment described by entry 8 using a simple malonate<sup>20</sup> substrate was conducted as a mechanistic control experiment in order to elucidate, if the catalyst is capable of controlling the stereocenter generated at the nitroolefin more or less independently from the formation of a stereocenter at the nucleophile. The configuration of the generated stereocenter is in fact the same as in the other cases thus demonstrating an efficient control over the electrophile trajectory and face differentiation.

The 1,4-addition is not limited to  $\beta$ -ketoesters and malonates, but could also be applied to a  $\gamma$ -lactam and a succinimide carrying an additional ester moiety (entries 9 & 10).

Moreover, the catalyst was applied to ketoester **1l** containing an enone moiety which could be used for a cascade Michael cyclization forming a bicyclic core, in which four contiguous stereocenters have been created (Scheme 3).

### Scheme 3. Application to a Cascade Cyclization.



**4** can also be considered as a formal [4+2]-cycloaddition product. Whereas the synthesis of diastereomer **4-D1** has already been described in literature,<sup>21</sup> an efficient access to **4-D2** was previously elusive. With 5 mol% of catalyst **C1b-Cu\*** product **4** was formed in high yield and with high diastereopreference for nearly enantiopure **4-D2**.

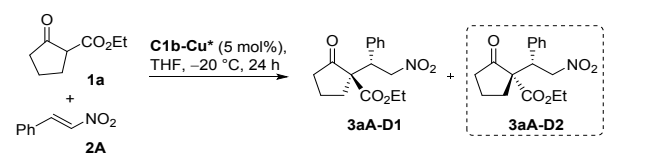
The intramolecular cyclization of the intermediate Michael addition product **31A** took largely place during the reaction time, but did not go to completion. For that reason, TBAF was added as a base after all nitroolefin had been consumed to finalize the formation of the bicyclic product. Addition of the base at this stage of the reaction did not have a negative influence on the stereoselectivity.

### Catalyst Recycling

An important practical aspect is the high robustness of the catalyst, which is neither particularly prone to air nor to moisture and can be readily recovered from the reaction mixture and reused for additional runs (Table 5). The catalyst was simply separated from the reaction mixture by filtration over silica gel. The zwitterionic catalyst is protonated on silica gel as is visible by the characteristic color change from red-brown to olive-green (see above and in the mechanistic investigations below). By washing with petroleum ether/ethylacetate (1:1) the product, starting materials, etc. were eluted whereas the charged precatalyst was sticking on the silica gel. Subsequent treatment of the silica pad with THF/CH<sub>2</sub>Cl<sub>2</sub>/NEt<sub>3</sub> (66:33:1) regenerated the betaine species, which was eluted and recovered in pure form as confirmed by ESI-MS and UV-Vis.

With reisolated catalyst the productivity maintained on a high level over at least four runs in terms of yield, diastereo- and enantioselectivity. After the 4<sup>th</sup> run 60% of the original catalyst amount was reisolated for the small reaction scale. In the 5<sup>th</sup> run yield and diastereoselectivity were still high, but started to decrease.

**Table 5. Repetitive Use of Recycled Catalyst.**



| run | yld.<br>(%) <sup>a</sup> | D1:D2 <sup>a</sup> | ee<br>(%) <sup>b</sup> |
|-----|--------------------------|--------------------|------------------------|
| 1   | 99                       | 6:94               | 99                     |
| 2   | 95                       | 6:94               | 98                     |
| 3   | 96                       | 6:94               | 98                     |
| 4   | 98                       | 5:95               | 98                     |
| 5   | 87                       | 7:93               | 98                     |

<sup>a</sup>Yield of isolated product after column chromatography. <sup>b</sup>Enantiomeric excess of **3aA-D2** determined by HPLC.

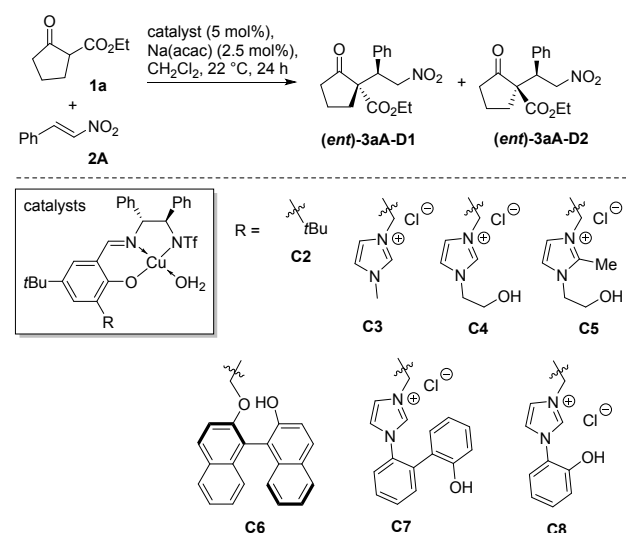
### Mechanistic Studies and Considerations

#### Control Systems

The results shown in Table 1 indicate a crucial role of the catalyst's betaine moiety. To further investigate its role, a number of control ligands were prepared and examined, which were lacking one or the other functional group in the residue R (Table 6). The structurally simplest complex **C2** carried a *tert*-butyl substituent. In the presence of base this complex is catalytically active (entry 1), but the inherently favored diastereomer D1 was formed in excess and in almost racemic form.<sup>22</sup> Installation of an imidazolium moiety in catalyst **C3** caused a switch of the diastereopreference, but the activity and

enantioselectivity were low (entry 2). The bifunctional imidazolium in **C4** carrying an aliphatic OH as protic moiety allowed for a similar diastereoselectivity, but a significantly better yield and enantioselectivity thus suggesting that an OH group is beneficial by hydrogen bond activation.<sup>23</sup> However, the enantio- and diastereoselectivity were considerably lower than with our standard catalyst system carrying a naphthol unit. In the absence of base **C4** was almost inactive under these conditions (8% yield, D1:D2 = 47:53, ee(D2) = 40%). Placing a methyl substituent at the imidazolium-2-position led to a loss in diastereoselectivity, whereas the enantioselectivity and activity were on a high level (entry 4). Both H-bond activation through the imidazolium's C(2)-H bond,<sup>24-26</sup> but also Coulomb interactions are thus likely to be involved in the activation process and stereocontrol.<sup>27</sup>

**Table 6. Investigation of Control Catalyst Systems.**



| #                | catalyst  | yield<br>(%) <sup>a</sup> | D1:D2 <sup>a</sup> | ee<br>(%) <sup>b</sup> |
|------------------|-----------|---------------------------|--------------------|------------------------|
| 1                | <b>C2</b> | 83                        | 80:20              | 5                      |
| 2                | <b>C3</b> | 30                        | 26:74              | 25                     |
| 3                | <b>C4</b> | 94                        | 28:72              | 76                     |
| 4                | <b>C5</b> | 88                        | 52:48              | 79                     |
| 5 <sup>c,d</sup> | <b>C6</b> | 84                        | 60:40              | 2                      |
| 6                | <b>C7</b> | 25                        | 17:83              | 95                     |
| 7 <sup>c,d</sup> | <b>C8</b> | 61                        | 6:94               | 97                     |

<sup>a</sup>Determined by <sup>1</sup>H NMR analysis of the crude product using mesitylene as an internal standard. <sup>b</sup>Enantiomeric excess of **(ent)-3aA-D2** determined by HPLC. Note that the iminotriflamide group has the opposite configuration than for **C1b-Cu** used above. <sup>c</sup>KOtBu (4.5 mol%) was used as a base instead of Na(acac). <sup>d</sup>Reaction was performed in THF.

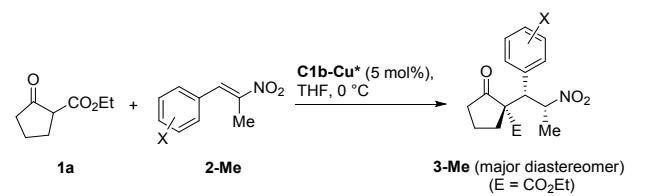
This conclusion is further substantiated by the use of an ether linked naphthol catalyst system **C6**, which provided the inherently favored diastereomer in excess. Interestingly, in this case D2 was almost racemic. For very high enantio- and diastereoselectivity both the imidazolium and an aromatic alcohol unit were necessary.

Next to our standard catalyst system also the structurally more simple complexes **C7** and **C8** containing phenol moieties provided the otherwise rare diastereomer with high selectivity.

### Formation of a Third Contiguous Stereocenter

Since the polyfunctional catalyst in its protonated form is expected to protonate a putative nitronate intermediate – formed in the C-C bond formation step– using its naphthol moiety, we were interested, if a third stereocenter could also be controlled when employing  $\alpha,\beta$ -disubstituted nitroolefins **2-Me**. Such asymmetric reactions between  $\beta$ -ketoesters and  $\alpha,\beta$ -disubstituted nitroolefins have never been reported before. Table 7 showcases that high stereoselectivity was indeed attained in this task.<sup>28</sup> One out of four possible diastereomers was formed in large excess and in nearly enantiopure form in all six examples. The absolute configuration of **3aA-Me** and **3aE-Me** was determined by X-ray crystal structure analysis.<sup>18</sup>

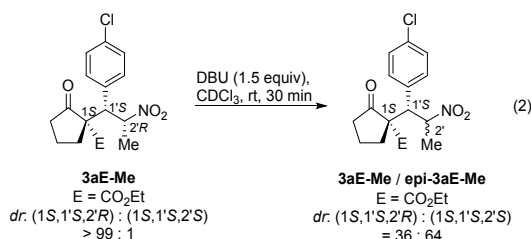
**Table 7. Control of a Third Stereocenter Using  $\alpha,\beta$ -Disubstituted Nitroolefins.**



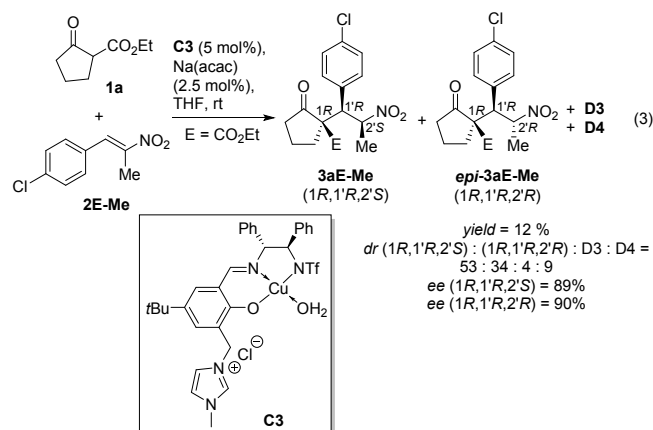
| # | X                         | <b>3-Me</b>   | yield (%) <sup>a</sup> | dr <sup>b</sup>        | ee (%) <sup>b,c</sup> |
|---|---------------------------|---------------|------------------------|------------------------|-----------------------|
| 1 | H                         | <b>3aA-Me</b> | 91                     | 94.3 : 3.0 : 2.0 : 0.7 | >99                   |
| 2 | <i>p</i> -Br              | <b>3aB-Me</b> | 92                     | 94.2 : 2.6 : 2.4 : 0.8 | >99                   |
| 3 | <i>m</i> -Br              | <b>3aC-Me</b> | 86                     | 96.6 : 1.9 : 1.3 : 0.2 | 99                    |
| 4 | <i>p</i> -Cl              | <b>3aE-Me</b> | 99                     | 93.8 : 2.9 : 2.9 : 0.4 | >99                   |
| 5 | <i>m</i> -NO <sub>2</sub> | <b>3aI-Me</b> | 88                     | 91.6 : 4.9 : 2.2 : 1.3 | >99                   |
| 6 | <i>p</i> -Me              | <b>3aK-Me</b> | 74                     | 93.4 : 4.2 : 2.3 : 0.1 | 98                    |

<sup>a</sup> Yield of isolated product after column chromatography. <sup>b</sup> Determined by HPLC from the crude product. <sup>c</sup> Enantiomeric excess for the major diastereomer.

To probe if the high diastereoselectivity might be a thermodynamic effect forming the most stable diastereomer, product **3aE-Me** was treated with DBU at room temperature (eq. 2). Rapid partial epimerization was observed resulting in an equilibrium mixture of **3aE-Me** and **epi-3aE-Me** with a ratio of 36 : 64. This shows that the stereocenter in  $\alpha$ -position to the nitro group was formed under kinetic control in the catalytic reaction.



In a further control experiment, the simplified catalyst **C3** lacking the naphtholate moiety was used (eq. 3). In that case the level of stereocontrol regarding the stereocenter created in the protonation step is poor affirming the role of the naphthol moiety in the protonation event. In addition the yield was poor.



The attained level of stereocontrol with the betaine catalyst **C1b-Cu\*** is unprecedented for a Michael addition to  $\alpha,\beta$ -disubstituted nitroolefins generating three contiguous stereocenters.<sup>28</sup>

### Kinetic Studies and Investigation of a Possible Non-Linear Effect

The initial reaction rate kinetics were investigated by <sup>1</sup>H-NMR. Using the differential method<sup>29</sup> the following empirical rate law was found for the model reaction in THF at room temperature (for details see the Supporting Information):

$$r = k * [\text{C1b-Cu}^*]^{0.93} * [\text{1a}]^{0.67} * [\text{2A}]^{0.96}$$

The initial rate  $r$  thus approximately shows a first-order kinetic dependence for the catalyst and the Michael acceptor. The observation of a ca. 2/3-order kinetic dependence for the pronucleophile **1a** might point to a partial substrate saturation.<sup>30b</sup>

Since the order in catalyst suggests that a single catalyst molecule is involved in the acceleration of the turnover-limiting step in the model reaction, the possibility of a non-linear effect was also investigated to confirm this interpretation.<sup>31</sup> Like expected, we found a strictly linear correlation between catalyst ee and product ee values (for details see the Supporting Information). In addition concentration dependent UV-Vis experiments have been performed which show a strictly linear correlation between concentration and absorbance (Beer's plot). These findings support the assumption that catalyst aggregates do not play an important role under the catalysis conditions.

Because analysis of the initial reaction rates is limited to relatively low conversions, the reaction progress kinetic



analysis (RPKA) method of Blackmond was also studied by  $^1\text{H-NMR}$  spectroscopy to receive information about the progress over the complete course of the catalytic reaction.<sup>30</sup> By the “same excess” protocol (see also the Supporting Information),<sup>30</sup> the same reaction is investigated starting from different points. Compared to a standard reference reaction (Figure 1, blue curve) the initial concentrations of substrates **1a** and **2A** in a second experiment (red curve) corresponded to those of the reference reaction experiment when the latter had reached 50% conversion.<sup>30</sup> In case of no catalyst decomposition or product inhibition, for both experiments the reaction progress from this point onward should be the same.<sup>30</sup>

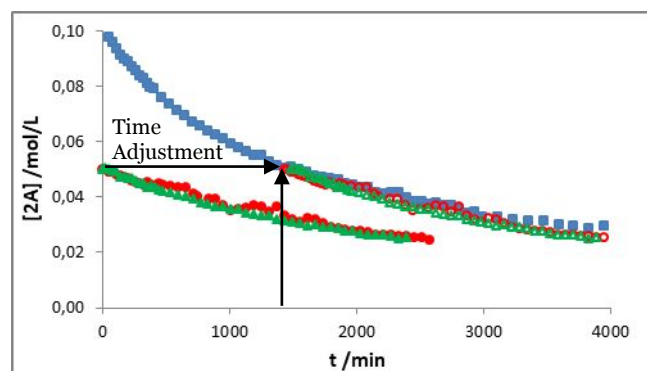


**Figure 1.** Reaction profiles of **2A** using Blackmond's “same excess” protocol<sup>30</sup> for probing catalyst stability and product influence (■: standard reaction, ●: 0.5 equiv. **1a** and **2A**, ▲ 0.5 equiv. **1a**, **2A** plus 0.5 equiv. product **3aA**; ○ and △: corresponding time adjusted profiles.)

Indeed, a good overlay of the “time-adjusted” curves of the kinetic profiles was observed, which indicates that no significant catalyst deactivation takes place and that the active catalyst concentration remains constant during the catalytic reaction. In a third “same-excess” experiment (green curve), the same starting point was used as in the second experiment (blue curve), but 50 mol% of product **3aA** was directly added from the start to the analyzed reaction mixture. Also in that case, a good overlay of the reaction profiles was obtained thus confirming that the product **3aA** does not significantly influence the catalyst during the product formation.

The variable time normalization analysis method (VTNA) described by Burés was used to elucidate the orders of the model reaction in all reaction components.<sup>32</sup>

Kinetic analysis monitoring **2A** made use of four reactions with different initial concentrations of **C1b-Cu\***, **1a** and **2A** (see Table 8, Figure 2 and the Supporting Information).

**Table 8.** Initial Concentrations of the Kinetic Experiments for Determining the Partial Orders of the Model Reaction.

| #  | Experiment | [ <b>1a</b> ]<br>/ mol/L | [ <b>2A</b> ]<br>/ mol/L | [ <b>C1b-Cu*</b> ]<br>/ mmol/L |
|----|------------|--------------------------|--------------------------|--------------------------------|
| K1 | standard   | 0.11                     | 0.10                     | 5.0                            |

|    |                          |      |      |     |
|----|--------------------------|------|------|-----|
| K2 | diff. [ <b>C1b-Cu*</b> ] | 0.11 | 0.10 | 2.5 |
| K3 | diff. [ <b>1a</b> ]      | 0.15 | 0.10 | 5.0 |
| K4 | diff. [ <b>2A</b> ]      | 0.11 | 0.15 | 5.0 |

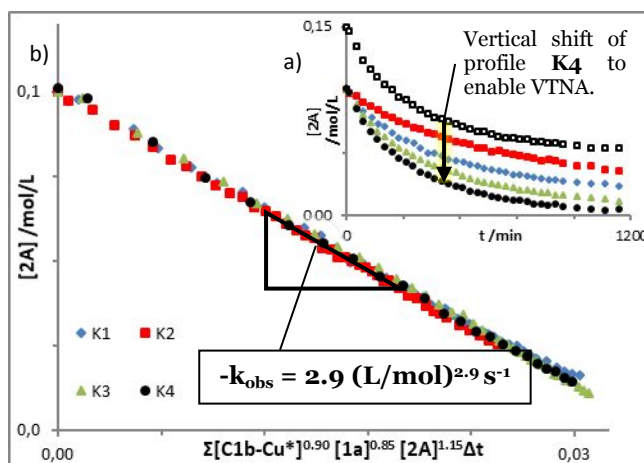


**Figure 2.** a) Conversion profile of the nitroolefin **2A** with different initial concentrations in **1a**, **2A** and **C1b-Cu\*** (see Table 7 for the color code). b) VTNA-profiles with x-axis normalization for [**C1b-Cu\***], [**1a**] and [**2A**]. Unit of the x-axis in  $(\text{mol/L})^{2.9} \text{s}$ .

Over the complete reaction course, the best overlay was achieved when partial orders of 0.90 for **C1b-Cu\***, 0.85 for **1a** and 1.15 for **2A** were used in the normalization of the time scale axis. Under the reaction conditions  $k_{\text{obs}}$  was found to be  $2.9 (\text{L/mol})^{2.9} \text{s}^{-1}$  (see Figure 2, b)). The following empirical rate law was thus found for the model reaction in THF at room temperature:

$$r = k_{\text{obs}} * [\text{C1b-Cu}^*]^{0.90} * [\text{1a}]^{0.85} * [\text{2a}]^{1.15}$$

Over the complete course the reaction rate  $r$  thus approximately shows a first-order kinetic dependence for the catalyst **C1b-Cu\*** and the Michael acceptor **2a**, in relatively good agreement with the empirical rate law determined from the initial reaction rates. The overall kinetic dependence for the pronucleophile **1a** of 0.85 is closer to 1 than for the initial reaction rate kinetics (0.67). However, taking a closer look, the order gradually changed during the course of the reaction from 0.7 at the beginning with  $\beta$  approaching a value of approximately 1 at the end of the reaction. Similar to Blackmond's work we explain the initial order between 0 and 1 with a partial substrate saturation.<sup>30b,33</sup> At higher conversions with decreasing ratios of substrate / catalyst, the substrate saturation will become less and less important. This is also in agreement with titration studies shown below. The dependence of the concentration of the catalyst and both substrates on the reaction rate could be explained with the C-C-bond formation as the rate determining step.

### Structural and Spectroscopic Studies

Unfortunately and despite extensive attempts an X-ray crystal structure analysis could so far not been obtained for the activated Cu(II) betaine catalysts like **C1b-Cu\***, or its precursor **C1b-Cu**. On the other hand, the related BINOL-based control system **C6** formed suitable crystals (Figure 3).<sup>34</sup> The crystal structure analysis confirmed the

assumed square planar coordination geometry, in which H<sub>2</sub>O serves as an additional ligand.

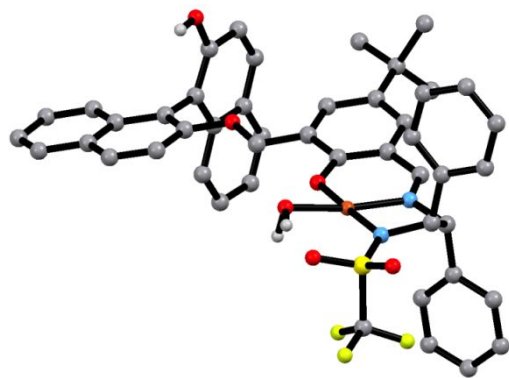


**Figure 3.** X-Ray crystal structure analysis of C6 (solvent molecules and H atoms have been omitted for clarity).

As mentioned above, the protonation state of the binaphthol(ate) moiety of the Cu(II) catalysts is already visible. Whereas the betaine **C1b-Cu\*** is red-brown colored, the naphthol precatalyst form **C1b-Cu** is dark olive-green. UV-Vis-NIR spectra of both species and of the free ligand are depicted in Figure 4/top.

Titration experiments were conducted in which the betaine form **C1b-Cu\*** was treated with ketoester **1a** (Figure 4 /bottom). With an increasing excess of ketoester, the amount of a new catalyst species was getting more and more dominant. An equilibrium is obviously formed, probably by Cu enolate formation including a proton transfer to the naphtholate function. Note that for technical reasons, the titrations needed to be performed at much lower concentrations than the catalytic reactions. The ketoester substrate and THF are expected to compete for the catalyst binding site. For that reason the dilution should have a strong influence on the equilibrium.

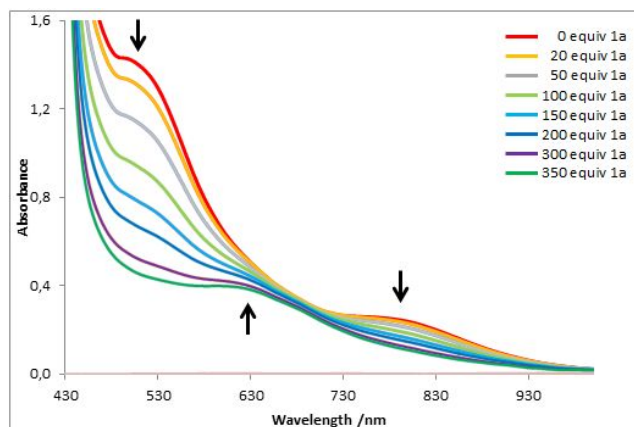
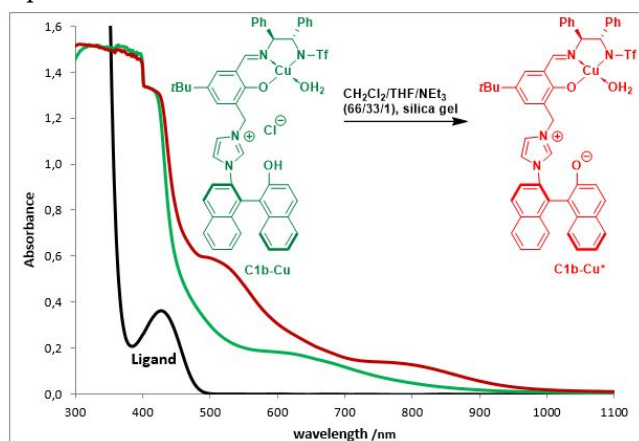


**Figure 4.** Top: UV-Vis-NIR spectra of **C1b-Cu\*** (red line), **C1b-Cu** (green line) and the free ligand (black line). Bottom: UV-Vis titration experiments adding ketoester **1a** to catalyst **C1b-Cu\***.

To get more information about this Cu(II) species EPR studies were conducted (Figure 5).

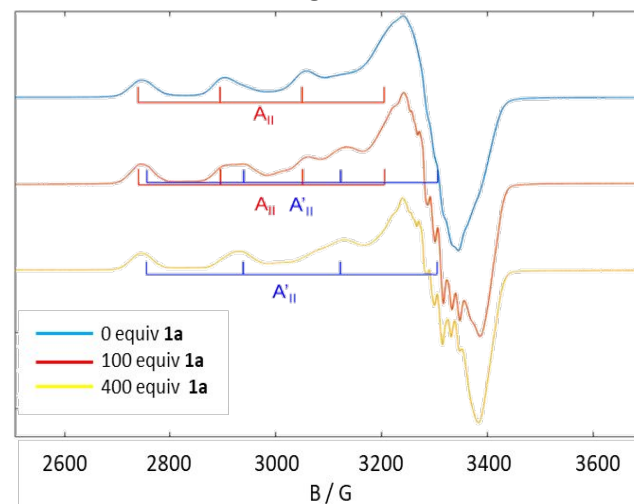


**Figure 5.** X-band EPR spectrum of **C1b-Cu\*** (blue), **C1b-Cu\*** plus 100 equiv of **1a** (red), and **C1b-Cu\*** plus 400 equiv **1a** (yellow) in THF at 108 K.

**C1b-Cu\*** and the unactivated form **C1b-Cu** both showed a typical Cu(II) axial signal in the X-band EPR spectrum at 108 K in THF under high dilution. The four lines in the parallel region arise from the hyperfine coupling of  $S = 1/2$  to copper nuclear spin  $I = 3/2$ . **C1b-Cu** showed  $g_{II} = 2.13$ ,  $A_{II} (63,65\text{Cu}) = 523 \text{ MHz}$  and  $g_I = 1.97$ ,  $A_I (63,65\text{Cu}) = 33 \text{ MHz}$  (see ESI) while **C1b-Cu\*** showed a shift in the  $g_{II} = 2.26$ ,  $A_{II} (63,65\text{Cu}) = 526 \text{ MHz}$  and  $g_I = 2.06$ ,  $A_I (63,65\text{Cu}) = 38 \text{ MHz}$  (Figure 5). The increase in the  $g$  value is typical for increased axial coordination around the Cu(II) center and is due to the change in ligand field and rigidity of the ligand.<sup>35</sup> Addition of nitroolefin to **C1b-Cu\*** did not cause any significant change to the EPR spectrum (see ESI). Addition of 100 equiv of **1a** resulted in a new signal to appear at  $g_{II} = 2.24$ ,  $A_{II} (63,65\text{Cu}) = 590 \text{ MHz}$  and  $g_I = 2.04$ ,  $A_I (63,65\text{Cu}) = 46 \text{ MHz}$  (Figure 5). After addition of 400 equiv of **1a** only the new signal could be detected (Figure 5). While the final spectrum shows better resolution of the  $A(^{14}\text{N})$ , this is due to dilution and reduced exchange broadening.<sup>36</sup> The EPR spectrum of

**C1b-Cu\*** plus 400 equiv. **1a** shows that a new species is generated, which is not **C1b-Cu**. Instead a more axial signal suggests the binding of **1a**.

### Calculations

The crystal structure of **C6** (Figure 3) served as a starting point to calculate optimized minimum energy structures of **C6** and the betaine catalyst in its naphthol form **C1b-Cu** (Figure 6). Having identified these structures, we explored the reaction mechanism of the catalytic cycle (Scheme 4) by calculating stationary points along the reaction pathway (minima as well as transition state structures; Figures 7 and S28 (see the SI)). The density functional theory (DFT) calculations were performed at the B3LYP<sup>37</sup> level of theory using the cc-pVDZ<sup>38</sup> basis set as implemented in the Gaussian 16 program package.<sup>39</sup> All structures were preoptimized in the gas phase and confirmed to be either true minima or true transition state structures by frequency calculations (zero or one imaginary frequency, respectively). We searched for the most stable conformers as a function of the binding motifs and torsion angles of the ligand. The structures were reoptimized using the IEF-PCM model<sup>40</sup> to include the self-consistent reaction field of the solvent (THF). We extracted and compared relative free Gibbs energies at 250 K. The presented structures are neutral (except **C1b-Cu**, which is a cation) and exhibit a multiplicity of 2. All calculations were performed in the electronic ground states.

In contrast to the solid state structure, two hydrogen bonds stabilize the molecular entities of **C6** and **C1b-Cu** (Figure 6) between (1) the naphthol OH and the water ligand and (2) between the water ligand and the sulfonyl moiety. These conformations were found to be more stable than the minimum structures with crystal-like conformations (stabilization of 6 and 14 kJ/mol for **C6** and **C1b-Cu**; details in the Supporting Information).

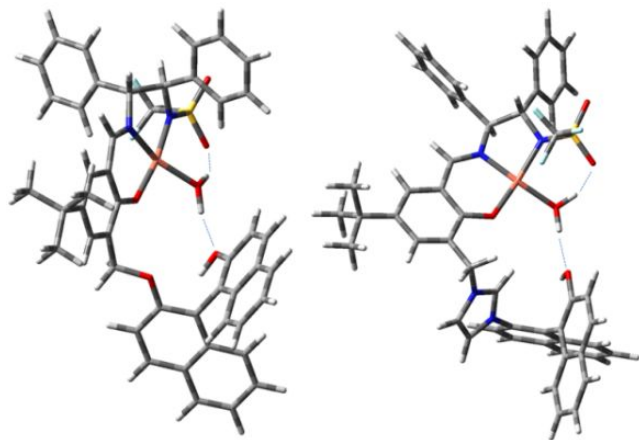


**Figure 6. Most stable conformations of the control system **C6** (left) and the precatalyst **C1b-Cu** (right): optimized structures by DFT calculations at the B3LYP/cc-pVDZ/IEF-PCM (THF) level of theory. The dotted blue lines indicate hydrogen bonding. Light gray: H; dark gray: C; dark blue: N; orange: Cu; light blue: F; yellow: S.**

A number of stationary points were identified along the reaction path and established an energy profile (Figures 7 and S28 (see the SI)) corresponding to the proposed

catalytic cycle (Scheme 4). The energies of all species within the energy profile are given relative to the energy sum of the free educts (nitroolefin and ketoester),  $\text{H}_2\text{O}$  and **C1b-Cu\*-THF**.

The reaction is initially triggered by the ketoester (in its keto form) replacing the  $\text{H}_2\text{O}$  ligand of **C1b-Cu\*** by coordinating to the copper center. This results in minimum structure **I(keto)** which adopts a coordination number of 5 at the copper(II) center. Both square pyramidal and trigonal bipyramidal metal geometries have been discussed in literature for Cu(II) catalysis employing bidentate substrates.<sup>41</sup> This pathway is endergonic and consumes 68 kJ/mol.

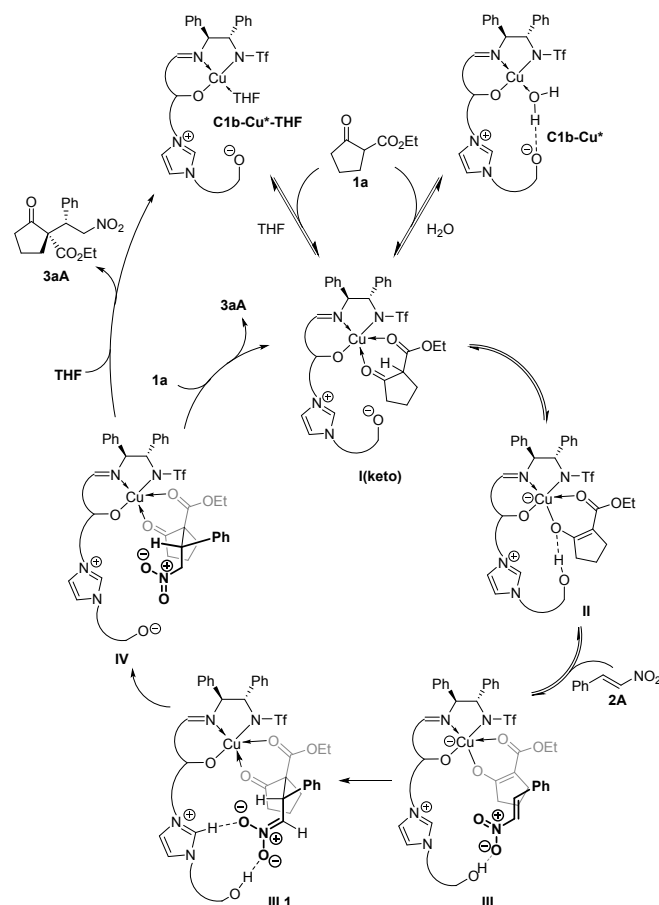
We also took into consideration that **C1b-Cu\*** may lose the  $\text{H}_2\text{O}$  ligand resulting in an intermediate structure **C1b-Cu\*(-H<sub>2</sub>O)**. The copper center stabilizes the naphtholate moiety by binding the ligand forming a distorted square planar coordination sphere. However, **C1b-Cu\*** is 23 kJ/mol more stable than **C1b-Cu\*(-H<sub>2</sub>O)**. **C1b-Cu\*** might serve as well as a starting point of the catalysis.

An exchange of the  $\text{H}_2\text{O}$  ligand with a THF ligand results in **C1b-Cu\*-THF**. It lacks any stabilizing intramolecular hydrogen bonds resulting in a higher reactivity than **C1b-Cu\***. However, the direct  $\text{H}_2\text{O}$  / THF ligand exchange requires 87 kJ/mol, *i.e.* more energy than is needed to form **I(keto)** or **C1b-Cu\*(-H<sub>2</sub>O)** from **C1b-Cu\***. It is more likely, that **C1b-Cu\*-THF** is formed after finishing a catalytic cycle by dissociation of the product from **IV**, facilitated by the solvent THF (to be discussed in the following).

The ketoester may then easily replace the THF ligand of **C1b-Cu\*-THF** coordinating to the copper center. This also results in the minimum structure **I(keto)**. This pathway is exergonic releasing 19 kJ/mol of energy.

**I(keto)** facilitates the exergonic formation of the next minimum structure along the pathway, Cu-enolate structure **II**. **II** exhibits a neutral naphthol OH group as well as the ketoester in its enolate form coordinated to the copper center. A hydrogen bond between these groups stabilizes this structure significantly. Consequently, it is the most stable structure within the proposed catalytic cycle (-57 kJ/mol). A rotation of the coordinated bidentate enolate by ca. 180° destabilizes the complex significantly (details in the Supporting Information). We found a transition state structure (**TS I(keto)/II**) connecting **I(keto)** and **II**. The virtual frequency vibration of **TS I(keto)/II** illustrates the proton migration from the keto CH group to the naphtholate O-group (cf. displacement vector in Figure S26, see Supporting Information). The activation barrier for this process is 19 kJ/mol.

**Scheme 4. Simplified Plausible Catalytic Mechanism. For structural details, transition state structures and energetics refer to Figures 7 and S28 (see SI).**



The naphthol OH group of **II** facilitates the barrierless bonding and activation of one nitroolefin molecule by OH / ONO hydrogen bonding ( $\text{OH}\cdots\text{O}$  distance: 1.650 Å) resulting in minimum structure **III**. This is an endergonic process consuming 21 kJ/mol due to the entropic penalty of **III** (free energy: -36 kJ/mol relative to the energy sum of the free educts and **C1b-Cu\***).

It follows the endergonic C-C-bond formation between the enolate and the activated nitroolefin resulting in minimum structure **III.1** (relative free energy of **III.1**: -4 kJ/mol). An OH / ONO hydrogen bond ( $\text{OH}\cdots\text{O}$  distance: 1.555 Å) stabilizes **III.1**. We found a transition

state structure (**TS III / III.1**, see Figures 7 & S28 in the SI) connecting **III** and **III.1**. The virtual frequency vibration of **TS III / III.1** illustrates the C-C-bond formation (cf. displacement vector in Figure S27 in the Supporting Information). **TS III / III.1** exhibits a hydrogen bond between the imidazolium C(2)-H<sup>5k,25,42</sup> and the nitro group ( $\text{CH}\cdots\text{O}$  distance: 1.877 Å). The finely tuned network of  $\text{OH}\cdots\text{O}$  and  $\text{CH}\cdots\text{O}$  hydrogen bonds as well as conceivable Coulomb interactions<sup>24b</sup> spatially preorganize the nitroolefin during the C-C-bond formation. In consequence, the catalyst can accomplish the otherwise rare relative product configuration of **3aA-D2**. This is in accord with our experimental observations as the presence of both the OH group and the imidazolium were crucial for high stereoselectivity (Table 6). The activation barrier for the C-C-bond formation is 70 kJ/mol (relative to **III**), which is the highest barrier of the catalytic cycle. The calculations thus suggest the C-C-bond formation as the rate-limiting event of the reaction, in agreement with the kinetic studies. This step is practically irreversible under the reaction conditions, because ee values and diastereoselectivities did not change upon prolonged reaction times.

A proton transfer from the naphthol group to the nitronate completes the product formation and results in minimum structure **IV**. The proton transfer is also an endergonic process consuming 28 kJ/mol (relative free energy of **IV**: 24 kJ/mol). A THF molecule, e.g., could then close the catalytic cycle by replacing and releasing the product. This results in structure **C1b-Cu\*-THF** as discussed above. Just releasing the product would result in the structure **C1b-Cu\*(-H2O)** as discussed above. Likewise, **1a** might displace the product leading directly to **I(keto)**.



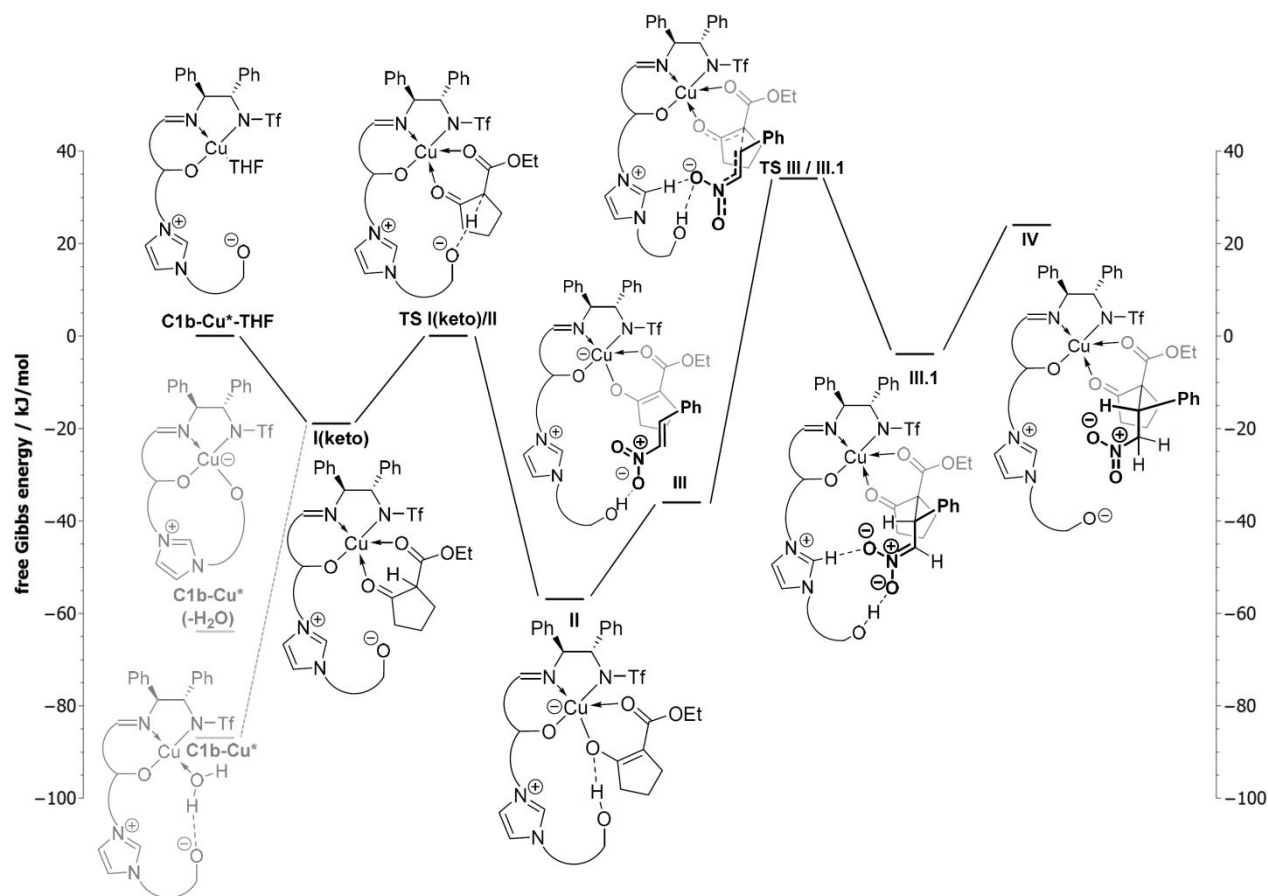


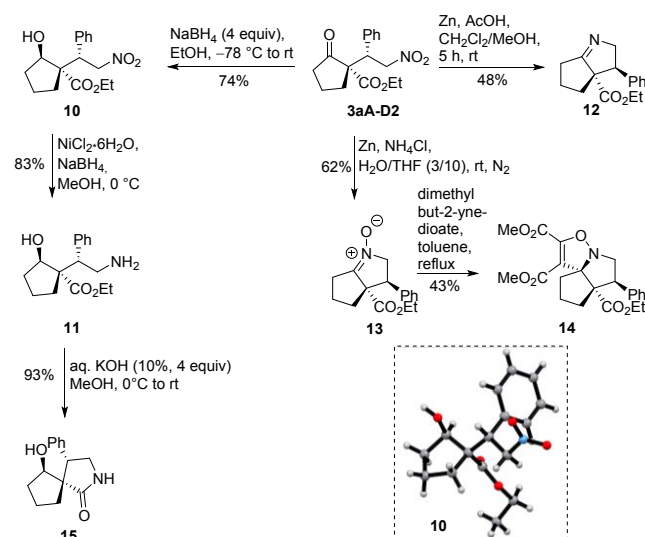
**Figure 7.** Free energy profile of the proposed catalytic cycle (cf. Scheme 4), which shows calculated stationary points (minima- and transition state structures) along the reaction coordinate. Free Gibbs energies at 250 K are relative to the energy sum of the free educts (nitroolefin and ketoester), H<sub>2</sub>O and the intermediate structure C1b-Cu\*-THF. The structures arise from DFT calculations at the B3LYP/cc-pVDZ/IEF-PCM (THF) level of theory. For structural details refer to Figure S28, see Supporting Information.

## Derivatization

To showcase the utility of the new diastereomeric product series, some further synthetic transformations were studied giving products that were previously not efficiently available with the depicted relative configurations (Scheme 5). In no case a partial epimerization was noticed. The chemoselective reduction of the keto group proceeded nearly fully diastereoselectively giving **10**. Its absolute configuration was determined by X-ray crystallography. Chemoselective reduction of the nitro moiety was then achieved with NaBH<sub>4</sub> in the presence of NiCl<sub>2</sub>\*6H<sub>2</sub>O providing  $\gamma$ -amino acid ester **11**,<sup>18</sup> which could be readily transformed into spiro lactam **15**.

Chemoselective reduction of the NO<sub>2</sub> group of **3aA-D2** with Zn/HOAc yielded the bicyclic imine **12**. In contrast, in the presence of NH<sub>4</sub>Cl nitron **13** was obtained.<sup>43</sup> The latter was applied to a thermal [3+2]-cycloaddition with an electron-poor dipolarophile to give the tricyclic spiro-compound **14**. The new tetrasubstituted stereocenter was formed with full diastereocontrol. Its configuration was determined by noesy (see SI).

## Scheme 5. Examples for possible application of **3aA-D2** to Synthesize Valuable Chiral Synthetic Building Blocks (in the Box: Solid State Structure of **10**).



## CONCLUSIONS

In conclusion, we have reported a new strategy for cooperative asymmetric catalysis, in which a Lewis acid works in concert with an imidazolium aryloxide betaine moiety within a polyfunctional chiral catalyst system. This system enabled for the first time an efficient general access to the otherwise rare diastereomeric product series for the direct 1,4-addition of various 1,3-dicarbonyl Michael donors to nitroolefins. Due to the robust nature of the catalyst and its peculiar zwitterionic nature, it can be readily recycled and reused. Control experiments revealed that both the imidazolium and the aryloxide are crucial to form the otherwise rare diastereomer in high yield and with high enantioselectivity. Kinetic studies including RPKA according to Blackmond and VTNA according to Burés, suggest that a single catalyst molecule is involved, which is stable and not inhibited by product, and that the C-C-bond formation is the turnover limiting event. This conclusion is further substantiated by DFT calculations of the catalytic cycle, which reveals the balanced interplay of the Cu(II) Lewis acid on the one hand, and the Brønsted basic naphtholate and different H-bonds on the other hand.

Notably, a third stereocenter could also be efficiently controlled in the 1,4-addition with  $\alpha,\beta$ -disubstituted nitroolefin substrates making use of a highly diastereoselective protonation of the nitronate intermediate. Asymmetric reactions between  $\beta$ -ketoesters and  $\alpha,\beta$ -disubstituted nitroolefins have not been reported before. The reaction scope could also be extended to a cascade cyclization providing a bicyclic densely functionalized building block with four contiguous stereocenters. Further applications of this novel catalyst type will be reported in due course.

## ASSOCIATED CONTENT

**Supporting Information.** This material is available free of charge via the Internet at <http://pubs.acs.org>.

Experimental details, spectral data, copies of  $^1\text{H}$  and  $^{13}\text{C}$  NMR spectra of all new compounds, and copies of HPLC traces (pdf), cif files for compounds **C6**, **3aA-D2**, **3aA-Me**, **3aB-D2**, **3aC-D2**, **3aE-D2**, **3aE-Me**, **3aF-D2**, **3aH-D2**, **3aJ-D2**, **3aK-D2**, **3cA-D2**, **3dA-D2**, **3hA-D2**, **10** and **11**).

## AUTHOR INFORMATION

### Corresponding Author

\* rene.peters@oc.uni-stuttgart.de

### Author Contributions

All authors have given approval to the final version of the manuscript.

### Notes

The authors declare no competing financial interest.

## ACKNOWLEDGMENT

This work was financially supported by the Deutsche Forschungsgemeinschaft (PE 818/7-1, project number 310990893). JL acknowledges support by the state of Baden-Württemberg through bwHPC and the German Research Foundation (DFG) through grant no INST 40/467-1 FUGG (JUSTUS cluster). We thank Mike D. Herrmann for the

preparation of several nitroolefin substrates and Konstantin Dorst for helpful discussions.

## ABBREVIATIONS

acac, acetylacetonate; BINAM, 1,1'-bi(2-naphthylamine); B3LYP, Becke 3 coefficients Lee Yang Parr; cc-pVTZ, correlation consistent split valence double zeta, DFT, density functional theory; IEF-PCM, integral equation formalism - polarizable continuum model; HPLC, high performance liquid chromatography; NIR, near infrared; NMR, nuclear magnetic resonance; TBAF, tetra-*n*-butylammonium fluoride; THF, tetrahydrofuran; UV, ultraviolet; vis, visible.

## REFERENCES

- Fersht, A. *Structure and Mechanism in Protein Science: A Guide to Enzyme Catalysis and Protein Folding*. W. H. Freeman, 1999.
- Fessner, W.-D.; Schneider, A.; Held, H.; Sinerius, G.; Walter, C.; Hixon, M.; Schloss, J. V. The Mechanism of Class 11, Metal-Dependent Aldolases, *Angew. Chem., Int. Ed. Engl.* **1996**, *35*, 2219.
- Lemke, T. L.; Williams, D. A.; Roche, V. F.; Zito S. W. (eds.), Foye's Principles of Medicinal Chemistry, 7<sup>th</sup> ed., Lippincott Williams & Wilkins, Wolters Kluwer, Baltimore, **2013**.
- Selected recent reviews: a) Lin, L.; Feng, X. Catalytic Strategies for Diastereodivergent Synthesis, *Chem. Eur. J.* **2017**, *23*, 6464; b) Bihani, M.; Zhao, J. C.-G. Advances in Asymmetric Diastereodivergent Catalysis, *Adv. Synth. Catal.* **2017**, *359*, 534; c) Beletskaya, I. P.; Nájera, C.; Yus, M. Stereodivergent Catalysis, *Chem. Rev.* **2018**, *118*, 5080; d) Krautwald, S.; Carreira, E. M. Stereodivergence in Asymmetric Catalysis, *J. Am. Chem. Soc.* **2017**, *139*, 5627.
- Selected leading examples: a) Wang, B.; Wu, F.; Wang, Y.; Liu, X.; Deng, L. Control of Diastereoselectivity in Tandem Asymmetric Reactions Generating Nonadjacent Stereocenters with Bifunctional Catalysis by Cinchona Alkaloids, *J. Am. Chem. Soc.* **2007**, *129*, 768; b) Wang, Y.; Li, H.; Wang, Y.-Q.; Liu, Y.; Foxman, B. M.; Deng, L. Asymmetric Diels-Alder Reactions of 2-Pyrones with a Bifunctional Organic Catalyst, *J. Am. Chem. Soc.* **2007**, *129*, 6364; c) Yan, X.-X.; Peng, Q.; Li, Q.; Zhang, K.; Yao, J.; Hou, X.-L.; Wu, Y.-D. Highly Diastereoselective Switchable Enantioselective Mannich Reaction of Glycine Derivatives with Imines, *J. Am. Chem. Soc.* **2008**, *130*, 14362; d) Nojiri, A.; Kumagai, N.; Shibasaki, M. Linking Structural Dynamics and Functional Diversity in Asymmetric Catalysis, *J. Am. Chem. Soc.* **2009**, *131*, 3779; e) Lu, G.; Yoshino, T.; Morimoto, H.; Matsunaga, S.; Shibasaki, M. Stereodivergent Direct Catalytic Asymmetric Mannich-Type Reactions of  $\alpha$ -Isothiocyanato Ester with Ketimines, *Angew. Chem., Int. Ed.* **2011**, *50*, 4382; f) Tian, X.; Cassani, C.; Liu, Y.; Moran, A.; Urakawa, A.; Galzerano, P.; Arceo, E.; Melchiorre, P. Diastereodivergent Asymmetric Sulfa-Michael Additions of  $\alpha$ -Branched Enones using a Single Chiral Organic Catalyst, *J. Am. Chem. Soc.* **2011**, *133*, 17934; g) Luparia, M.; Oliveira, M. T.; Audisio, D.; Frébault, F.; Goddard, R.; Maulide, N. Catalytic Asymmetric Diastereodivergent Deracemization, *Angew. Chem., Int. Ed.* **2011**, *50*, 12631; h) McInturff, E. L.; Yamaguchi, E.; Krische, M. J. Chiral-Anion-Dependent Inversion of Diastereo- and Enantioselectivity in Carbonyl Crotylation via Ruthenium-Catalyzed Butadiene Hydrohydroxyalkylation, *J. Am. Chem. Soc.* **2012**, *134*, 20628; i) Eitel, S. H.; Jautze, S.; Frey, W.; Peters, R. Asymmetric Michael Additions of  $\alpha$ -Cyanoacetates by Soft Lewis Acid / Hard Brønsted Acid Catalysis: Stereodivergency With Bi- vs Monometallic Catalysts, *Chem. Sci.* **2013**, *4*, 2218; j) Krautwald, S.; Schafroth, M. A.; Sarlah, D.; Carreira, E. M. Stereodivergent  $\alpha$ -Allylation of Linear Aldehydes with Dual Iridium and Amine Catalysis, *J. Am. Chem. Soc.* **2014**, *136*, 3020; k) Mechler, M.; Peters, R. Diastereodivergent Asymmetric 1,4-Addition of Oxindoles to Nitroolefins by Using Polyfunctional Nickel-Hydrogen-Bond-Azolium Catalysts,

*Angew. Chem. Int. Ed.* **2015**, *54*, 10303; l) Shi, S.-L.; Wong, Z. L.; Buchwald, S. L. Copper-catalysed enantioselective stereodivergent synthesis of amino alcohols, *Nature* **2016**, *532*, 353; m) Zhan, G.; Shi, M.-L.; He, Q.; Lin, W.-J.; Ouyang, Q.; Du, W.; Chen, Y.-C. Catalyst-Controlled Switch in Chemo- and Diastereoselectivities: Annulations of Morita-Baylis-Hillman Carbonates from Isatins, *Angew. Chem., Int. Ed.* **2016**, *55*, 2147; n) Uraguchi, D.; Yoshioka, K.; Ooi, T. Complete diastereodivergence in asymmetric 1,6-addition reactions enabled by minimal modification of a chiral catalyst, *Nat. Commun.* **2017**, *8*, 14793; o) Zheng, H.; Wang, Y.; Xu, C.; Xu, X.; Lin, L.; Liu, X.; Feng, X. Stereodivergent synthesis of vicinal quaternary-quaternary stereocenters and bioactive hyperolactones, *Nat. Commun.* **2018**, *9*, 1968.

<sup>6</sup> Comprehensive review: Zheng, K.; Liu, X.; Feng, X. Recent Advances in Metal-Catalyzed Asymmetric 1,4-Conjugate Addition (ACA) of Nonorganometallic Nucleophiles, *Chem. Rev.* **2018**, *118*, 7586.

<sup>7</sup> Selected reviews about 1,4-additions: a) Kanai, M.; Shibasaki, M. in *Catalytic Asymmetric Synthesis*, 2nd ed. (Ed.: Ojima, I.), Wiley: New York, **2000**; pp 569-592; b) Christoffers, J.; Baro, A. Construction of Quaternary Stereocenters: New Perspectives through Enantioselective Michael Reactions, *Angew. Chem., Int. Ed.* **2003**, *42*, 1688; c) Christoffers, J.; Koripelly, G.; Rosiak, A.; Rössler, M. Recent Advances in Metal-Catalyzed Asymmetric Conjugate Additions, *Synthesis* **2007**, 1279; d) Jautze, S.; Peters, R. Catalytic Asymmetric Michael Additions of  $\alpha$ -Cyanoacetates, *Synthesis* **2010**, 365.

<sup>8</sup> Selected examples: a) Li, H.; Wang, Y.; Tang, L.; Wu, F.; Liu, X.; Guo, C.; Foxman, B. M.; Deng, L. Stereocontrolled Creation of Adjacent Quaternary and Tertiary Stereocenters by a Catalytic Conjugate Addition, *Angew. Chem., Int. Ed.* **2005**, *44*, 105; b) Okino, T.; Hoashi, Y.; Furukawa, T.; Xu, X.; Takemoto, Y. Enantio- and Diastereoselective Michael Reaction of 1,3-Dicarbonyl Compounds to Nitroolefins Catalyzed by a Bifunctional Thiourea, *J. Am. Chem. Soc.* **2005**, *127*, 119; c) Malerich, J. P.; Hagihara, K.; Rawal, V. H. Chiral Squaramide Derivatives are Excellent Hydrogen Bond Donor Catalysts, *J. Am. Chem. Soc.* **2008**, *130*, 14416; d) Chen, Z.; Furutachi, M.; Kato, Y.; Matsunaga, S.; Shibasaki, M. A Stable Homodinuclear Biscobalt(III)-Schiff Base Complex for Catalytic Asymmetric 1,4-Addition Reactions of  $\beta$ -Keto Esters to Alkynones, *Angew. Chem., Int. Ed.* **2009**, *48*, 2218; e) Yu, Z. P.; Liu, X. H.; Zhou, L.; Lin, L. L.; Feng, X. M. Bifunctional Guanidine via an Amino Amide Skeleton for Asymmetric Michael Reactions of  $\beta$ -Ketoesters with Nitroolefins: A Concise Synthesis of Bicyclic  $\beta$ -Amino Acids, *Angew. Chem., Int. Ed.* **2009**, *48*, 5195; f) Kwon, K.; Kim, D. Y. Organocatalytic Asymmetric Michael Addition of  $\beta$ -Ketoesters to Nitroalkenes, *Bull. Korean Chem. Soc.* **2009**, *30*, 1441; g) Furutachi, M.; Chen, Z.; Matsunaga, S.; Shibasaki, M. Catalytic Asymmetric 1,4-Additions of  $\beta$ -Keto Esters to Nitroalkenes Promoted by a Bifunctional Homobimetallic Co<sub>2</sub>-Schiff Base Complex, *Molecules* **2010**, *15*, 532; h) Bae, H. Y.; Some, S.; Oh, J. S.; Lee, Y. S.; Song, C. E. Hydrogen bonding mediated enantioselective organocatalysis in brine: significant rate acceleration and enhanced stereoselectivity in enantioselective Michael addition reactions of 1,3-dicarbonyls to  $\beta$ -nitroolefins, *Chem. Commun.* **2011**, 47, 9621; i) Li, X.; Li, X.; Peng, F.; Shao, Z. Mutually Complementary Metal- and Organocatalysis with Collective Synthesis: Asymmetric Conjugate Addition of 1,3-Carbonyl Compounds to Nitroalkynes and Further Reactions of the Products, *Adv. Synth. Catal.* **2012**, *354*, 2873; j) Chen, J.; Huang, Y. Asymmetric catalysis with *N*-heterocyclic carbenes as non-covalent chiral templates, *Nat. Commun.* **2014**, *5*, 3437.

<sup>9</sup> a) Ono, N. *The Nitro Group in Organic Synthesis*; Wiley-VCH: New York, **2001**; b) Ballini, R.; Petrini, M. Recent synthetic developments in the nitro to carbonyl conversion (Nef reaction), *Tetrahedron* **2004**, *60*, 1017.

<sup>10</sup> Selected examples for the use of addition reactions of Michael donors to nitroolefins in the inherently favored product

synthesis: a) Jakubec, P.; Cockfield, D. M.; Dixon, D. J. Total Synthesis of (–)-Nakadomarin A, *J. Am. Chem. Soc.* **2009**, *131*, 16632; b) Jakubec, P.; Hawkins, A.; Felzmann, W.; Dixon, D. J. Total Synthesis of Manzamine A and Related Alkaloids, *J. Am. Chem. Soc.* **2012**, *134*, 17482; c) Kyle, A. F.; Jakubec, P.; Cockfield, D. M.; Cleator, E.; Skidmore, J.; Dixon, D. J. Total synthesis of (–)-nakadomarin A, *Chem. Commun.* **2011**, 47, 10037; d) Jakubec, P.; Kyle, A. F.; Calleja, J.; Dixon, D. J. Total synthesis of (–)-nakadomarin A: alkyne ring-closing metathesis, *Tetrahedron Lett.* **2011**, *52*, 6094; e) Andrey, O.; Vidonne, A.; Alexakis, A. Organocatalytic Michael addition, a convenient tool in total synthesis. First asymmetric synthesis of (–)-botryodiplodin, *Tetrahedron Lett.* **2003**, *44*, 7901; f) Pansare, S. V.; Lingampally, R.; Kirby, R. L. Stereoselective Synthesis of 3-Aryloctahydroindoles and Application in a Formal Synthesis of (–)-Pancracine, *Org. Lett.* **2010**, *12*, 556; g) Ishikawa, H.; Suzuki, T.; Hayashi, Y. High-Yielding Synthesis of the Anti-Influenza Neuramidase Inhibitor (–)-Oseltamivir by Three “One-Pot” Operations, *Angew. Chem., Int. Ed.* **2009**, *48*, 1304; h) Hoashi, Y.; Yabuta, T.; Takemoto, Y. Bifunctional thiourea-catalyzed enantioselective double Michael reaction of  $\gamma,\delta$ -unsaturated  $\beta$ -ketoester to nitroalkene: asymmetric synthesis of (–)-epibatidine, *Tetrahedron Lett.* **2004**, *45*, 9185; i) Elsner, P.; Jiang, H.; Nielsen, J. B.; Pasi, F.; Jørgensen, K. A. A modular and organocatalytic approach to  $\gamma$ -butyrolactone autoregulators from Streptomyces, *Chem. Commun.* **2008**, 5827; j) Xu, G.-Q.; Lin, G.-Q.; Sun, B.-F. Concise asymmetric total synthesis of (–)-patchouli alcohol, *Org. Chem. Front.* **2017**, *4*, 2031.

<sup>11</sup> Note that in ref. 8f the relative configuration depicted for the products was erroneous (Kim, D., personal communication, May 10, 2018).

<sup>12</sup> For pioneering work on the general concept of cooperative Lewis acid / Brønsted base catalysis, see e.g.: a) Shibasaki, M.; Kumagai, N. Lewis acid–Brønsted base catalysis, in *Cooperative Catalysis – Designing Efficient Catalysts for Synthesis*; R. Peters (Ed.), Wiley-VCH, Weinheim, **2015**; b) Shibasaki, M.; Yoshikawa, N. Lanthanide Complexes in Multifunctional Asymmetric Catalysis, *Chem. Rev.* **2002**, *102*, 2187; c) Sasai, H.; Suzuki, T.; Arai, S.; Arai, T.; Shibasaki, M. Basic character of rare earth metal alkoxides. Utilization in catalytic carbon-carbon bond-forming reactions and catalytic asymmetric nitroaldol reactions, *J. Am. Chem. Soc.* **1992**, *114*, 4418; d) Sasai, H.; Arai, T.; Satow, Y.; Houk, K. N.; Shibasaki, M. The First Heterobimetallic Multifunctional Asymmetric Catalyst, *J. Am. Chem. Soc.* **1995**, *117*, 6194; e) Emori, E.; Arai, T.; Sasai, H.; A Catalytic Michael Addition of Thiols to  $\alpha,\beta$ -Unsaturated Carbonyl Compounds: Asymmetric Michael Additions and Asymmetric Protonations, Shibasaki, M. *J. Am. Chem. Soc.* **1998**, *120*, 4043; f) Yoshikawa, N.; Yamada, Y. M. A.; Das, J.; Sasai, H.; Shibasaki, M. Direct Catalytic Asymmetric Aldol Reaction, *J. Am. Chem. Soc.* **1999**, *121*, 4168; g) Yamaguchi, N.; Qin, H.; Matsunaga, S.; Shibasaki, M. Lewis Acid–Lewis Acid Heterobimetallic Cooperative Catalysis: Mechanistic Studies and Application in Enantioselective Aza-Michael Reaction, *J. Am. Chem. Soc.* **2005**, *127*, 13419; h) Gnanadesikan, V.; Horiuchi, Y.; Ohshima, T.; Shibasaki, M. Direct Catalytic Asymmetric Aldol-Tishchenko Reaction, *J. Am. Chem. Soc.* **2004**, *126*, 7782; i) Kim, Y. S.; Matsunaga, S.; Das, J.; Sekine, A.; Ohshima, T.; Shibasaki, M. Stable, Storable, and Reusable Asymmetric Catalyst: A Novel La-linked-BINOL Complex for the Catalytic Asymmetric Michael Reaction, *J. Am. Chem. Soc.* **2000**, *122*, 6506; j) Nemoto, T.; Ohshima, T.; Yamaguchi, K.; Shibasaki, M. Catalytic Asymmetric Epoxidation of Enones Using La–BINOL–Triphenylarsine Oxide Complex: Structural Determination of the Asymmetric Catalyst, *J. Am. Chem. Soc.* **2001**, *123*, 2725; k) Tokunaga, M.; Larrow, J. F.; Kakiuchi, F.; Jacobsen, E. N. Asymmetric catalysis with water: efficient kinetic resolution of terminal epoxides by means of catalytic hydrolysis, *Science* **1997**, *277*, 936; l) Reddy, J. M.; Jacobsen, E. N. Asymmetric Catalytic Synthesis of  $\alpha$ -Aryloxy Alcohols: Kinetic Resolution of Terminal Epoxides via Highly Enantioselective

Ring-Opening with Phenols, *J. Am. Chem. Soc.* **1999**, *121*, 6086; m) Schaus, S. E.; Brandes, B. D.; Larrow, J. F.; Tokunaga, M.; Hansen, K. B.; Gould, A. E.; Furrow, M. E.; Jacobsen, E. N. Highly Selective Hydrolytic Kinetic Resolution of Terminal Epoxides Catalyzed by Chiral (salen)Co<sup>III</sup> Complexes. Practical Synthesis of Enantioenriched Terminal Epoxides and 1,2-Diols, *J. Am. Chem. Soc.* **2002**, *124*, 1307; n) DiMauro, E. F.; Kozlowski, M. C. BINOL–Salen Metal Catalysts Incorporating a Bifunctional Design, *Org. Lett.* **2001**, *3*, 1641; o) DiMauro, E. F.; Kozlowski, M. C. Copper(II) Complexes of Novel 1,5-Diaza-*cis*-decalin Diamine Ligands: An Investigation of Structure and Reactivity, *Organometallics* **2002**, *21*, 1454; p) Annamalai, V.; DiMauro, E. F.; Carroll, P. J.; Kozlowski, M. C. Catalysis of the Michael Addition Reaction by Late Transition Metal Complexes of BINOL-Derived Salens, *J. Org. Chem.* **2003**, *68*, 1973; q) Handa, S.; Gnanadesikan, V.; Matsunaga, S.; Shibasaki, M. *syn*-Selective Catalytic Asymmetric Nitro-Mannich Reactions Using a Heterobimetallic Cu–Sm–Schiff Base Complex, *J. Am. Chem. Soc.* **2007**, *129*, 4900; r) Handa, S.; Gnanadesikan, V.; Matsunaga, S.; Shibasaki, M. Heterobimetallic Transition Metal/Rare Earth Metal Bifunctional Catalysis: A Cu/Sm/Schiff Base Complex for *Syn*-Selective Catalytic Asymmetric Nitro-Mannich Reaction, *J. Am. Chem. Soc.* **2010**, *132*, 4925; s) Handa, S.; Nagawa, K.; Sohtome, Y.; Matsunaga, S.; Shibasaki, M. A Heterobimetallic Pd/La/Schiff Base Complex for *anti*-Selective Catalytic Asymmetric Nitroaldol Reactions and Applications to Short Syntheses of  $\beta$ -Adrenoceptor Agonists, *Angew. Chem., Int. Ed.* **2008**, *47*, 3230; t) Sohtome, Y.; Kato, Y.; Handa, S.; Aoyama, N.; Nagawa, K.; Shibasaki, M. Stereodivergent Catalytic Doubly Diastereoselective Nitroaldol Reactions Using Heterobimetallic Complexes, *Org. Lett.* **2008**, *10*, 2231; u) Trost, B. M.; Ito, H. A Direct Catalytic Enantioselective Aldol Reaction via a Novel Catalyst Design, *J. Am. Chem. Soc.* **2000**, *122*, 12003.

<sup>13</sup> For pioneering research on ammonium phenolate betaine catalysis by the Ooi research group, see: a) Uruguchi, D.; Koshimoto, K.; Ooi, T. Chiral Ammonium Betaines: A Bifunctional Organic Base Catalyst for Asymmetric Mannich-Type Reaction of  $\alpha$ -Nitrocarboxylates, *J. Am. Chem. Soc.* **2008**, *130*, 10878; b) Uruguchi, D.; Koshimoto, K.; Ooi, T. Flexible synthesis, structural determination, and synthetic application of a new C<sub>1</sub>-symmetric chiral ammonium betaine, *Chem. Commun.* **2010**, *46*, 300; c) Uruguchi, D.; Koshimoto, K.; Miyake, S.; Ooi, T. Chiral Ammonium Betaines as Ionic Nucleophilic Catalysts, *Angew. Chem. Int. Ed.* **2010**, *49*, 5567; d) Uruguchi, D.; Koshimoto, K.; Ooi, T. Ionic Nucleophilic Catalysis of Chiral Ammonium Betaines for Highly Stereoselective Aldol Reaction from Oxindole-Derived Vinylic Carbonates, *J. Am. Chem. Soc.* **2012**, *134*, 6972; e) Uruguchi, D.; Oyaizu, K.; Ooi, T. Nitroolefins as a Nucleophilic Component for Highly Stereoselective Aza Henry Reaction under the Catalysis of Chiral Ammonium Betaines, *Chem. Eur. J.* **2012**, *18*, 8306; f) Oyaizu, K.; Uruguchi, D.; Ooi, T. Vinylogy in nitronates: utilization of  $\alpha$ -aryl conjugated nitroolefins as a nucleophile for a highly stereoselective aza-Henry reaction, *Chem. Commun.* **2015**, *51*, 4437.

<sup>14</sup> Chianese, A. R.; Crabtree, R. H. Axially Chiral Bidentate N-Heterocyclic Carbene Ligands Derived from BINAM: Rhodium and Iridium Complexes in Asymmetric Ketone Hydrosilylation, *Organometallics* **2005**, *24*, 4432.

<sup>15</sup> a) Mechler, M.; Latendorf, K.; Frey, W.; Peters, R. Homo- and Heterobimetallic Pd–, Ag–, and Ni–Hybrid Salen–Bis-NHC Complexes, *Organometallics* **2013**, *32*, 112; b) Mechler, M.; Frey, W.; Peters, R. Macrocyclic Salen–Bis-NHC Hybrid Ligands and Their Application to the Synthesis of Enantiopure Bi- and Trimetallic Complexes, *Organometallics* **2014**, *33*, 5492.

<sup>16</sup> For related ligand syntheses, see e.g.: a) Kull, T.; Peters, R. Contact Ion Pair (CIP) Directed Lewis-Acid Catalysis: Asymmetric Formation of *trans*-Configured  $\beta$ -Lactones, *Angew. Chem., Int. Ed.* **2008**, *47*, 5461; b) Kull, T.; Cabrera, J.; Peters, R. Catalytic Asymmetric Synthesis of *trans*-Configured  $\beta$ -Lactones: Cooperation of Lewis Acid and Ion Pair Catalysis,

*Chem. Eur. J.* **2010**, *16*, 9132; c) Meier, P.; Broghammer, F.; Latendorf, K.; Rauhut, G.; Peters, R. Cooperative Al(Salen)-Pyridinium Catalysts for the Asymmetric Synthesis of *trans*-Configured  $\beta$ -Lactones by [2+2]-Cyclocondensation of Acylbromides and Aldehydes: Investigation of Pyridinium Substituent Effects, *Molecules* **2012**, *17*, 7121; d) Broghammer, F.; Brodbeck, D.; Junge, T.; Peters, R. Cooperative Lewis acid–onium salt catalysis as tool for the desymmetrization of meso-epoxides, *Chem. Commun.* **2017**, *53*, 1156; e) Brodbeck, D.; Broghammer, F.; Meisner, J.; Klepp, J.; Garnier, D.; Frey, W.; Kästner, J.; Peters, R. An Aluminum Fluoride Complex with an Appended Ammonium Salt as an Exceptionally Active Cooperative Catalyst for the Asymmetric Carboxycyanation of Aldehydes, *Angew. Chem., Int. Ed.* **2017**, *56*, 4056; f) Latendorf, K.; Mechler, M.; Schamne, I.; Mack, D.; Frey, W.; Peters, R. Titanium Salen Complexes with Appended Silver NHC Groups as Nucleophilic Carbene Reservoir for Cooperative Asymmetric Lewis Acid / NHC Catalysis, *Eur. J. Org. Chem.* **2017**, *28*, 4140; g) Schmid, J.; Frey, W.; Peters, R. Polynuclear Enantiopure Salen–Mesoionic Carbene Hybrid Complexes, *Organometallics* **2017**, *36*, 4313; h) J. Schmid, T. Junge, J. Lang, W. Frey, R. Peters, *Angew. Chem. Int. Ed.* **2019**, *58*, 5447.

<sup>17</sup> The relative and absolute configuration of products **3aA-D2**, **3aA-Me**, **3aB-D2**, **3aC-D2**, **3aE-D2**, **3aE-Me**, **3aF-D2**, **3aH-D2**, **3aJ-D2**, **3aK-D2**, **3cA-D2**, **3dA-D2**, **3hA-D2**, **10** and **11** were determined by X-ray single crystal structure analysis. The absolute configuration of all other products **3A-D2** was assigned in analogy. Their relative configurations were assigned by comparison to literature or, if no data were available, in analogy (see the Supporting Information).

<sup>18</sup> Supplementary crystallographic data for **3aA-D2** (1872231), **3aA-Me** (1908072), **3aB-D2** (1872225), **3aC-D2** (1872232), **3aE-D2** (1872234), **3aE-Me** (1908073), **3aF-D2** (1872233), **3aH-D2** (1872227), **3aJ-D2** (1872224), **3aK-D2** (1872235), **3cA-D2** (1872236), **3dA-D2** (1872229) and **3hA-D2** (1872230), **10** (1872237) and **11** (1908074) have been deposited with the Cambridge Crystallographic Data Centre. Their deposition numbers are given in brackets. This material is available free of charge via the Internet at <http://pubs.acs.org> and <http://www.ccdc.cam.ac.uk/products/csd/request/>.

<sup>19</sup> For few acyclic products, the preferred formation of diastereomer D2 has already been reported to proceed with low to moderate diastereoselectivity, but the preference for diastereomer **3-D2** was not generally found in these studies. See e.g.: a) Okino, T.; Hoashi, Y.; Furukawa, T.; Xu, X.; Takemoto, Y. Enantio- and Diastereoselective Michael Reaction of 1,3-Dicarbonyl Compounds to Nitroolefins Catalyzed by a Bifunctional Thiourea, *J. Am. Chem. Soc.* **2005**, *127*, 119; b) Andrés, J. M.; Ceballos, M.; Maestro, A.; Sanz, I.; Pedrosa, R. Supported bifunctional thioureas as recoverable and reusable catalysts for enantioselective nitro-Michael reactions, *Beilstein J. Org. Chem.* **2016**, *12*, 628; c) Andrés, J. M.; Losada, J.; Maestro, A.; Rodríguez-Ferrer, P.; Pedrosa, R. Supported and Unsupported Chiral Squaramides as Organocatalysts for Stereoselective Michael Additions: Synthesis of Enantiopure Chromenes and Spirochromanes, *J. Org. Chem.* **2017**, *82*, 8444.

<sup>20</sup> a) Ji, J.; Barnes, D. M.; Zhang, J.; King, S. A.; Wittenberger, S. J.; Morton, H. Catalytic Enantioselective Conjugate Addition of 1,3-Dicarbonyl Compounds to Nitroalkenes, *J. Am. Chem. Soc.* **1999**, *121*, 10215; b) Li, H.; Wang, Y.; Tang, L.; Deng, L. Highly Enantioselective Conjugate Addition of Malonate and  $\beta$ -Ketoester to Nitroalkenes: Asymmetric C–C Bond Formation with New Bifunctional Organic Catalysts Based on Cinchona Alkaloids, *J. Am. Chem. Soc.* **2004**, *126*, 9906.

<sup>21</sup> Li, Y.; Wang, J.; Sun, W.; Shan, Y.; Sun, B.; Lin, G.; Zou, J. Enantioselective synthesis of bicyclo[2.2.2]octane-1-carboxylates under metal free conditions, *Org. Chem. Front.* **2015**, *2*, 274.

<sup>22</sup> The ee value of the major diastereomer D1 was 1% (not shown in the Table 6).



<sup>23</sup> Overview of hydrogen bonds in cooperative catalysis: Lu, X.; Deng, L. Hydrogen bonding-mediated cooperative organocatalysis by modified cinchona alkaloids in *Cooperative Catalysis*, R. Peters (Ed.), Wiley-VCH, Weinheim, **2015**.

<sup>24</sup> Recent reviews describing CH $\cdots$ X hydrogen bonds using azolium salts as H-bond donors: a) Cai, J.; Sessler, J. L. Neutral CH and cationic CH donor groups as anion receptors, *Chem. Soc. Rev.* **2014**, 43, 6198; b) Schulze, B.; Schubert, U. S. Beyond click chemistry – supramolecular interactions of 1,2,3-triazoles, *Chem. Soc. Rev.* **2014**, 43, 2522; c) general review on hydrogen bonds: Pihko, P. M., *Hydrogen Bonding in Organic Chemistry*, Wiley-VCH, Weinheim, **2009**.

<sup>25</sup> Ohmatsu, K.; Kiyokawa M.; Ooi, T. Chiral 1,2,3-Triazoliums as New Cationic Organic Catalysts with Anion-Recognition Ability: Application to Asymmetric Alkylation of Oxindoles, *J. Am. Chem. Soc.* **2011**, 133, 1307.

<sup>26</sup> For applications of 1,2,3-triazolium salts as enantioselective catalysts, see e.g. also: a) Ohmatsu, K.; Hamajima, Y.; Ooi, T. Catalytic Asymmetric Ring Openings of Meso and Terminal Aziridines with Halides Mediated by Chiral 1,2,3-Triazolium Silicates, *J. Am. Chem. Soc.* **2012**, 134, 8794; b) Ohmatsu, K.; Goto, A.; Ooi, T. Catalytic asymmetric Mannich-type reactions of  $\alpha$ -cyano  $\alpha$ -sulfonyl carbanions, *Chem. Commun.* **2012**, 48, 7913; c) Ohmatsu, K.; Furukawa, Y.; Kiyokawa, M.; Ooi, T. Diastereo- and enantioselective phase-transfer alkylation of 3-substituted oxindoles with racemic secondary alkyl halides, *Chem. Commun.* **2017**, 53, 13113.

<sup>27</sup> Selected reviews on asymmetric onium salt catalysis: a) Shirakawa, S.; Maruoka, K. Recent Developments in Asymmetric Phase-Transfer Reactions, *Angew. Chem., Int. Ed.* **2013**, 52, 4312; b) Maruoka, K. Practical Aspects of Recent Asymmetric Phase-Transfer Catalysis, *Org. Proc. Res. Dev.* **2008**, 12, 679.

<sup>28</sup> For other asymmetric 1,4-additions to  $\alpha,\beta$ -disubstituted nitroolefins see: formation of 3 stereocenters: a) Duschmale, J.; Wennemers, H., Adapting to Substrate Challenges: Peptides as Catalysts for Conjugate Addition Reactions of Aldehydes to  $\alpha,\beta$ -Disubstituted Nitroolefins, *Chem. Eur. J.* **2012**, 18, 1111; formation of 2 stereocenters: b) Kimmel, K. L.; Weaver, J. D.; Ellman, J. A. Enantio- and diastereoselective addition of cyclohexyl Meldrum's acid to  $\beta$ - and  $\alpha,\beta$ -disubstituted nitroalkenes via N-sulfinyl urea catalysis, *Chem. Sci.* **2012**, 3, 121; c) Wu, R.-H.; Chang, X.-F.; Lu, A.-D.; Wang, Y.-M.; Wu, G.-P.; Song, H.-B.; Zhou, Z.-H.; Tang, C. Chiral (thio)phosphorodiamides as excellent hydrogen bond donor catalysts in the asymmetric Michael addition of 2-hydroxy-1,4-naphthoquinone to nitroolefins, *Chem. Commun.* **2011**, 47, 5034.

<sup>29</sup> Pilling, M. J.; Seakins, P. W. *Reaction Kinetics*, Oxford University Press: Oxford, **1995**.

<sup>30</sup> a) Baxter, R. D.; Sale, D.; Engle, K. M.; Yu, J.-Q.; Blackmond, D. G. Mechanistic rationalization of unusual kinetics in Pd-catalyzed C-H olefination, *J. Am. Chem. Soc.* **2012**, 134, 4600; b) Blackmond, D. G. Kinetic Profiling of Catalytic Organic Reactions as a Mechanistic Tool, *J. Am. Chem. Soc.* **2015**, 137, 10852.

<sup>31</sup> Satyanarayana, T.; Abraham, S.; Kagan, H. B. Nonlinear Effects in Asymmetric Catalysis, *Angew. Chem., Int. Ed.* **2009**, 48, 456.

<sup>32</sup> a) Burés, J. Variable Time Normalization Analysis: General Graphical Elucidation of Reaction Orders from Concentration Profiles, *Angew. Chem., Int. Ed.* **2016**, 55, 16084; b) Nielsen, C. D.-T.; Burés, J. Visual kinetic analysis, *Chem. Sci.* **2019**, 10, 348; c) Aikonen, S.; Muuronen, M.; Wirtanen, T.; Heikkinen, S.; Musgreave, J.; Burés, J.; Helaja, J. Gold(I)-Catalyzed 1,3-O-Transposition of Ynones: Mechanism and Catalytic Acceleration with Electron-Rich Aldehydes, *ACS Catal.* **2018**, 8, 960.

<sup>33</sup> Zotova, N.; Broadbelt, L. J.; Armstrong, A.; Blackmond, D. G. Kinetic and mechanistic studies of proline-mediated direct intermolecular aldol reactions, *Bioorg. & Med. Chem. Lett.* **2009**, 19, 3934.

<sup>34</sup> Supplementary crystallographic data for **C6** have been deposited with the Cambridge Crystallographic Data Centre as deposition 1872223. This material is available free of charge via the Internet at <http://pubs.acs.org> and <http://www.ccdc.cam.ac.uk/products/csd/request/>.

<sup>35</sup> a) Damaj, Z.; Cisnetti, F.; Dupont, L.; Henon, E.; Policar, C.; Guillon, E. Synthesis, characterization and dioxygen reactivity of copper(I) complexes with glycoligands, *Dalton Trans.* **2008**, 3235; b) Sakaguchi, U.; Addison, A. W. Spectroscopic and redox studies of some copper(II) complexes with biomimetic donor atoms: implications for protein copper centres, *J. Chem. Soc., Dalton Trans.* **1979**, 600.

<sup>36</sup> Weil, J. A.; Bolton, J. R., *Electron Paramagnetic Resonance*, John Wiley & Sons, Inc.: **2006**.

<sup>37</sup> a) Miehl, B.; Savin, A.; Stoll, H.; Preuss, H. Results obtained with the correlation energy density functionals of Becke and Lee, Yang and Parr, *Chem. Phys. Lett.* **1989**, 157, 200; b) Becke, A. D. *J. Chem. Phys.* **1993**, 98, 5648.

<sup>38</sup> Dunning, T. H. Gaussian basis sets for use in correlated molecular calculations. I. The atoms boron through neon and hydrogen, *J. Chem. Phys.* **1989**, 90, 1007.

<sup>39</sup> Gaussian 16, Revision B.01, Frisch, M. J.; Trucks, G. W.; Schlegel, H. B.; Scuseria, G. E.; Robb, M. A.; Cheeseman, J. R.; Scalmani, G.; Barone, V.; Petersson, G. A.; Nakatsuji, H.; Li, X.; Caricato, M.; Marenich, A. V.; Bloino, J.; Janesko, B. G.; Gomperts, R.; Mennucci, B.; Hratchian, H. P.; Ortiz, J. V.; Izmaylov, A. F.; Sonnenberg, J. L.; Williams-Young, D.; Ding, F.; Lipparini, F.; Egidi, F.; Goings, J.; Peng, B.; Petrone, A.; Henderson, T.; Ranasinghe, D.; Zakrzewski, V. G.; Gao, J.; Rega, N.; Zheng, G.; Liang, W.; Hada, M.; Ehara, M.; Toyota, K.; Fukuda, R.; Hasegawa, J.; Ishida, M.; Nakajima, T.; Honda, Y.; Kitao, O.; Nakai, H.; Vreven, T.; Throssell, K.; Montgomery, Jr., J. A.; Peralta, J. E.; Ogliaro, F.; Bearpark, M. J.; Heyd, J. J.; Brothers, E. N.; Kudin, K. N.; Staroverov, V. N.; Keith, T. A.; Kobayashi, R.; Normand, J.; Raghavachari, K.; Rendell, A. P.; Burant, J. C.; Iyengar, S. S.; Tomasi, J.; Cossi, M.; Millam, J. M.; Klene, M.; Adamo, C.; Cammi, R.; Ochterski, J. W.; Martin, R. L.; Morokuma, K.; Farkas, O.; Foresman, J. B.; Fox, D. J. *Gaussian, Inc.*, Wallingford CT, **2016**.

<sup>40</sup> Tomasi, J.; Mennucci, B.; Cammi, R. Quantum Mechanical Continuum Solvation Models, *Chem. Rev.* **2005**, 105, 2999.

<sup>41</sup> Evans, D. A.; Burgey, C. S.; Kozlowski, M. C.; Tregay, S. W. C<sub>2</sub>-Symmetric Copper(II) Complexes as Chiral Lewis Acids. Scope and Mechanism of the Catalytic Enantioselective Aldol Additions of Enolsilanes to Pyruvate Esters, *J. Am. Chem. Soc.* **1999**, 121, 686.

<sup>42</sup> Reviews on hydrogen bonds in catalysis: a) Schreiner, P. R.; Metal-free organocatalysis through explicit hydrogen bonding interactions, *Chem. Soc. Rev.* **2003**, 32, 289; b) Doyle, A. G.; Jacobsen, E. N. Small-Molecule H-Bond Donors in Asymmetric Catalysis, *Chem. Rev.* **2007**, 107, 5713.

<sup>43</sup> The reaction was performed in analogy to Zhao, Y.; Wang, X.-J.; Lin, Y.; Cai, C.-X.; Liu, J.-T. Highly enantioselective direct Michael addition of 1,3-dicarbonyl compounds to  $\beta$ -fluoroalkyl- $\alpha$ -nitroalkenes, *Tetrahedron* **2014**, 70, 2523.

